the general science journal

Inconsistencies in EM Theory - the Kelvin Polarization Force Density Contradiction

Zoltan Losonc[1]

v. 1.2 (29.10.2018)

Abstract

Calculations of resultant electrostatic force on a charged spherical or cylindrical capacitor with two sectors of different dielectrics, based on the classical formulas of electrostatic pressure, Kelvin polarization force density, and Maxwell stress tensor predict a reactionless force that violates Newton's 3rd law. Measurements didn't confirm the existence of such a reactionless thrust, thus there is an apparent inconsistency in the classical EM theory that leads to wrong results.

Keywords: Dielectrophoresis, liquid dielectrophoresis, L-DEP, DEP, electrostatic pressure, Kelvin polarization force, Korteweg-Helmholtz, Maxwell stress tensor, anomaly, contradiction, paradox, inconsistency, electromagnetic theory, electrostatics, cylindrical capacitor, spherical capacitor, reactionless force, thrust, E-field thruster, inhomogeneous electric field, high voltage, torsion pendulum.

1 Introduction

When there are no electric charges on the external surface of a completely closed but internally charged spherical or cylindrical capacitor, then all internal electrostatic forces supposed to mutually cancel one another, and produce a zero resultant thrust, according to Newton's law of action and reaction.

If we calculate the resultant electrostatic force in simple cylindrical or spherical capacitors, an inexplicable contradiction emerges. When the dielectrophoretic forces are calculated using the classical equations of electrostatic forces on elementary dipoles, then the presence of a reactionless resultant thrust is predicted on the capacitor, violating Newton's 3rd law. The same result is obtained based on Kelvin polarization force density as well. The calculation method according to the divergence of Maxwell stress tensor yields a different, but still non-zero reactionless thrust. Only the methods based on the Maxwell surface stress tensor, and Korteweg-Helmholtz equation produce correct results for the whole capacitor, ie. zero resultant thrust; but the location and character of force components are incorrect in these cases.

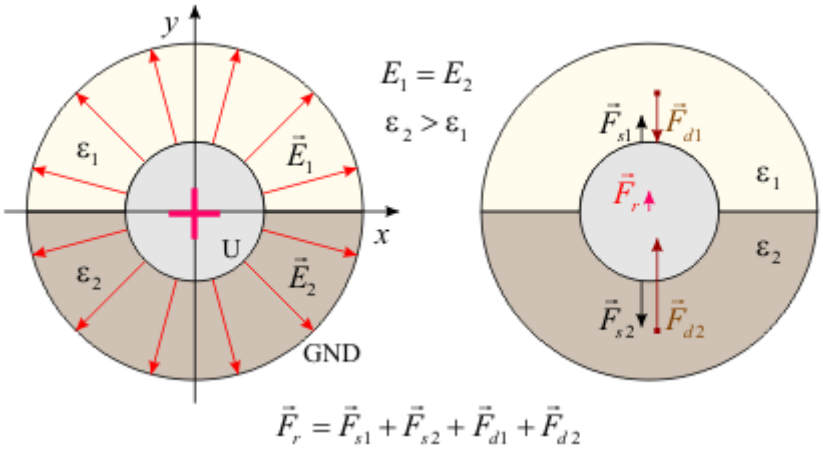

Figure 1: The cross section of the cylindrical capacitor filled with two different dielectrics, and force components.

[1] feprinciples@protonmail.com

This contradiction has been found and analyzed in spherical and cylindrical capacitors, but it is present in some other geometries as well, where Kelvin polarization forces exist due to the presence of inhomogeneous E-fields. The capacitor does not have to be perfectly concentric or coaxial in order to observe these effects in it, and its shape may also differ from a perfect sphere or perfect cylinder (ex. elliptical, or egg shaped etc.). Even though we describe capacitors filled with two 180° sectors of dielectrics having different permittivities, the observations are valid also when more than two dielectrics are used in more than two sectors, and/or when the sector angles are not equal. The boundaries between the dielectrics don't have to be exactly radial either.

In order to simplify the calculations, the analyzed coaxial cylindrical capacitor is assumed to be infinitely long, without free ends, and thus having no scattered E-fields. This ideal theoretical assumption can be well approximated by bending a long coaxial capacitor in a circle and merging the two free ends, forming a torus. If the diameter of the cylinder is much smaller than the radius of the torus, then it can be well approximated as a straight coaxial capacitor without free ends.

In these calculations we assume that ideal dielectrics are used, which are linear, isotropic, and homogeneous, containing no space charge. Electrostrictive phenomena are also neglected, and the permittivity assumed to be independent of pressure. The dielectric's electrical conductivity is assumed to be zero. The applied E-field intensities have to be below the breakdown strength of the dielectrics. Despite all these assumed ideal simplification, the import and conclusions of this paper may be valid for capacitors using nonlinear, anisotropic, imperfect dielectrics with significant conductivity, and included space charge, including electrostrictive materials as well.

Even though in scientific literature there is a distinction between the dielectrophoretic forces on solid dielectric particles surrounded by a second dielectric medium, and ponderomotive body forces that act on fluids (called liquid dielectrophoresis), their underlying basic physical principles are the same. Therefore, we will refer to such forces simply as dielectrophoretic (or Kelvin) forces, independent of the material's phase. The analysis of a spherical geometry would yield slightly simpler equations, but since the physical fabrication of a cylindrical capacitor prototype is easier, the discussions in this paper will focus on the cylindrical geometry.

2 The Resultant Electrostatic Force on a Cylindrical Capacitor With Two Different Dielectrics

2.1 The Necessary Condition of Satisfying Newton's 3rd Law

We can already conclude from Figure 1 without any calculations that in order to satisfy Newton's law of action-reaction, the resultant forces upon the upper ($\vec{F}_{r1} = \vec{F}_{s1} + \vec{F}_{d1}$) and lower domains should have identical magnitudes, pointing in opposite directions ($\vec{F}_{r1} = -\vec{F}_{r2}$). If this condition would not be satisfied, then a reactionless force would act on the capacitor, which would be very useful for spacecraft propulsion. The resultant forces on the two domains can have identical magnitudes only if they are independent of the dielectric's permittivity. In other words, the dielectrophoretic forces should exactly cancel the increased electrostatic pressure caused by increased permittivity.

2.2 Deriving the Equations of the Resultant Thrust

Let's calculate the resultant electrostatic force acting upon a coaxial cylindrical capacitor filled with two isotropic linear dielectrics of different permittivity as the function of an applied DC voltage. Based on Newton's 3rd law it is expected that this force should be zero, because there is no external electric field on the outer surface of the capacitor. However, as it turned out, the calculations predicted the presence of a non-zero resultant reactionless electrostatic force on it.

The capacitor is analyzed in 2D, assuming that its length (perpendicular to the plane of drawing) is infinite. Half of the space between the cylinders (a 180° sector) is filled with the first dielectric of permittivity ε_1, and the other half with another dielectric of permittivity ε_2 Figure 1. Despite the presence of two different dielectrics, the electric field is axially symmetric, pointing in radial direction, and its intensity varies only radially. This E-field distribution can be derived from the boundary conditions at the boundary surface between the two dielectrics, where the tangential E-field components in both dielectrics must be identical. The same conclusion can be drawn using the Gauss law as well. The orientation and intensity of the E-field is identical with the case of a coaxial cylindrical capacitor having only vacuum between the electrodes, and charged with a constant DC voltage U.

There are two different force types in the capacitor. One is the electrostatic pressure force $\vec{F}_s$ acting upon the conductor-dielectric boundary surfaces; and the other type is the dielectrophoretic force $\vec{F}_d$ acting upon the bulk of the dielectrics due to the presence of inhomogeneous electric fields. These force components have

different magnitudes in the two dielectric domains, therefore we have to calculate them separately for each domain. The resultant force is the sum of four components: two boundary surface components, and two volume force components $\vec{F}_r = \vec{F}_{s1} + \vec{F}_{s2} + \vec{F}_{d1} + \vec{F}_{d2}$.

2.2.1 Force Components of Electrostatic Pressure

Due to the axisymmetrical E-field distribution, the surface charge density on a conductor-dielectric boundary is constant within a sector of homogeneous dielectric (but it is greater on the inner electrode than on the outer one). The surface charge densities depend on the dielectric constant, and they are different in the two sectors. Therefore we have to calculate the electrostatic pressure components for each domain separately. Let's calculate the y component of the electrostatic pressure forces in the upper sector of the capacitor according to Figure 2 first. Even though in this calculation the bottom half is ignored, its presence is implicitly implied in order to maintain the axisymmetrical E-field distribution.

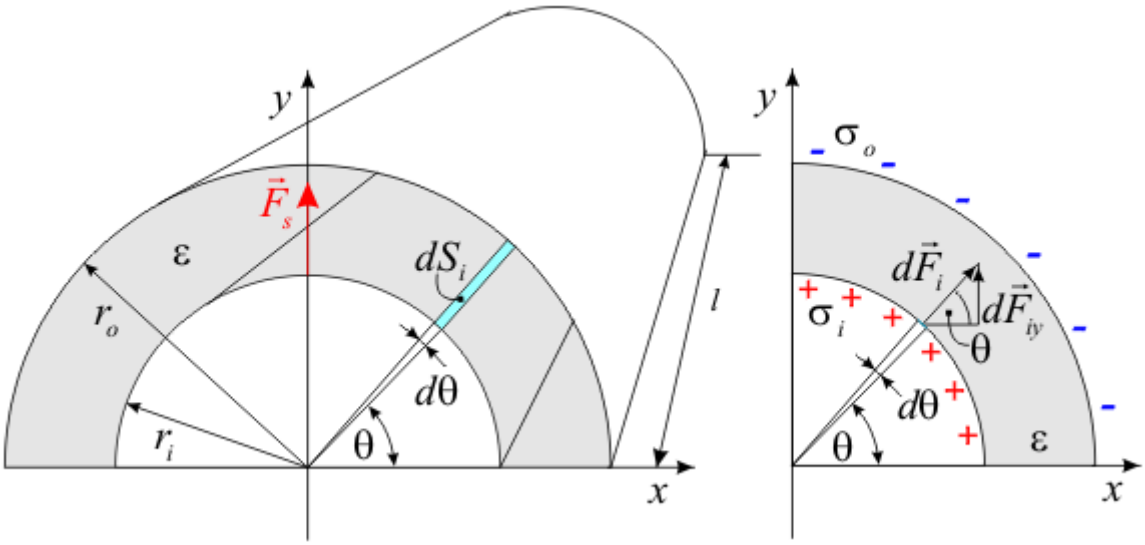

Figure 2: Calculating the y component of electrostatic pressure forces in the top 180° sector.

The E-field intensity in the dielectric has got only radial component, which is:

$$\boxed{E = \frac{U}{r \ln \frac{r_o}{r_i}}} \tag{1}$$

The equation of the surface charge density σ_i as the function of voltage U on the inner electrode can be derived from the correlation between the surface charge density and E-field intensity on the surface of a perfect conductor as:

$$E = \frac{\sigma}{\varepsilon}; \qquad \frac{\sigma_i}{\varepsilon} = \frac{U}{r_i \ln \frac{r_o}{r_i}}; \qquad \rightarrow \qquad \sigma_i = \frac{U\varepsilon}{r_i \ln \frac{r_o}{r_i}}$$

where r_o is the radius of outer electrode; r_i- radius of the inner electrode. The corresponding equation on the outer electrode can be obtained in similar way:

$$\sigma_o = \frac{U\varepsilon}{r_o \ln \frac{r_o}{r_i}}$$

The y component of the resultant electrostatic pressure force on the top 180° sector of inner electrode can be calculated (based on the equation of the electrostatic pressure on a conductor $f = \frac{\sigma^2}{2\varepsilon}$) by integrating the y components of elementary forces $d\vec{F}_i$ acting on elementary surfaces dS_i, as shown on Figure 2:

$$d\vec{F}_i = f_i dS_i \hat{\boldsymbol{r}}; \quad dS_i = l r_i d\theta; \quad d\vec{F}_i = \frac{\sigma_i^2 l r_i d\theta}{2\varepsilon_1}\hat{\boldsymbol{r}}$$

$$dF_{iy} = dF_i \sin\theta = \frac{\sigma_i^2 l r_i}{2\varepsilon_1} \sin\theta d\theta$$

$$dF_{iy} = \frac{U^2 \varepsilon_1^2 l r_i}{2\varepsilon_1 r_i^2 \left(\ln \frac{r_o}{r_i}\right)^2} \sin\theta d\theta = \frac{\varepsilon_1 U^2 l}{2 r_i \left(\ln \frac{r_o}{r_i}\right)^2} \sin\theta d\theta$$

$$F_{iy} = \int_{\theta=0}^{\pi} dF_{iy} = \frac{\varepsilon_1 U^2 l}{2 r_i \left(\ln \frac{r_o}{r_i}\right)^2} \int_{\theta=0}^{\pi} \sin\theta d\theta = \frac{\varepsilon_1 U^2 l}{2 r_i \left(\ln \frac{r_o}{r_i}\right)^2} [-\cos\theta]_0^{\pi}$$

$$F_{iy} = \frac{\varepsilon_1 U^2 l}{r_i \left(\ln \frac{r_o}{r_i}\right)^2}$$

The corresponding equation for the outer electrode can be obtained in similar way:

$$F_{oy} = -\frac{\varepsilon_1 U^2 l}{r_o \left(\ln \frac{r_o}{r_i}\right)^2} \tag{2}$$

The resultant electrostatic pressure force upon the top 180° sector of the capacitor is the sum of inner and outer components ($\hat{\boldsymbol{y}}$ - unit vector in y direction):

$$F_{s1y} = F_{iy} + F_{oy} = \frac{\varepsilon_1 U^2 l}{\left(\ln \frac{r_o}{r_i}\right)^2} \left(\frac{1}{r_i} - \frac{1}{r_o}\right)$$

$$\boxed{\vec{F}_{s1} = \frac{\varepsilon_1 \left(r_o - r_i\right) U^2 l}{r_i r_o \left(\ln \frac{r_o}{r_i}\right)^2} \hat{\boldsymbol{y}}} \tag{3}$$

2.2.2 Dielectrophoretic Force Components - Based on Elementary Dipoles

Besides the above calculated electrostatic pressure force, there is another force type in the cylindrical capacitor, the dielectrophoretic force that acts upon the bulk of dielectric due to the presence of inhomogeneous electric field. This force component is the result of unequal electric forces upon the positive and negative charges of neutral molecular dipoles in an inhomogeneous E-field. It can be calculated in several ways using generally accepted equations presented in scientific textbooks and related literature. Let's calculate the dielectrophoretic force component in the top 180° sector based on a direct approach first, by integrating the infinitesimal electric forces upon the elementary dipoles of the dielectric (Figure 3).

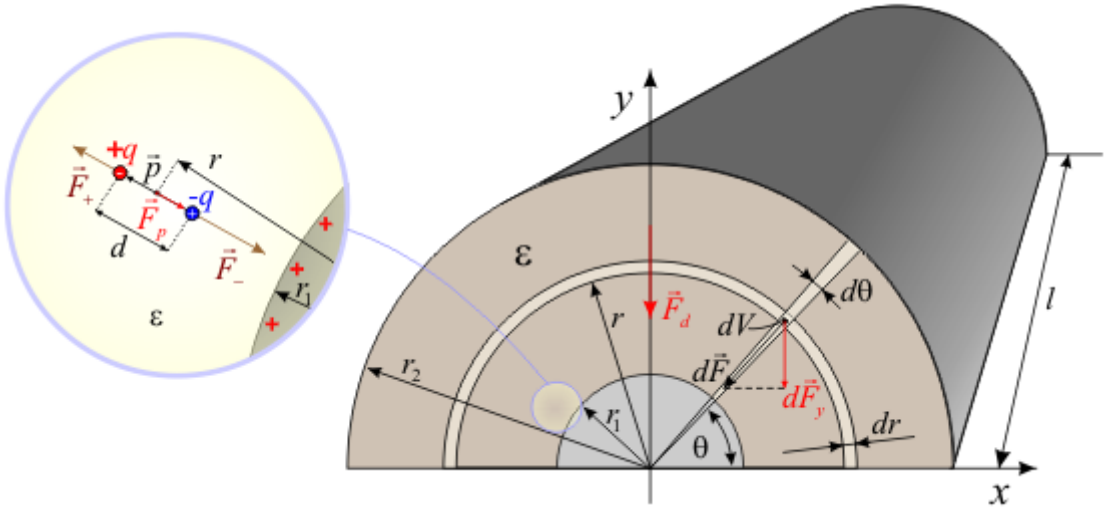

Figure 3: Calculating the dielectrophoretic force component on the bulk of dielectric.

First we have to calculate the attracting and repelling electrostatic forces upon the positive and negative charges of an elementary dipole. Then by summing up the two opposing forces we get the resultant force upon

an elementary dipole. The macroscopic resultant dielectrophoretic force component is obtained by integrating the y components of the elementary forces over the whole volume of a single dielectric.

For these calculations, we have to know the magnitude of the equivalent dipole moment $d\vec{p}$ of an infinitesimal volume dV of polarized dielectric as the function of the local E-field intensity. In the case of linear isotropic dielectrics this can be calculated from the equation:

$$\vec{P} = N\vec{p} = \frac{n\vec{p}}{V}$$

where $\vec{P}$ is the electric polarization (volumetric density of dipoles); n - number of dipoles; V - volume; N - density of dipoles; $\vec{p}$ - dipole moment. The correlation between P and E is:

$$D = \varepsilon E = \varepsilon_0 E + P \quad \rightarrow \quad P = E\left(\varepsilon - \varepsilon_0\right)$$

The dipole moment of an infinitesimal volume of dielectric is:

$$dp = PdV; \qquad dp = E\left(\varepsilon - \varepsilon_0\right)dV$$

Now we can calculate the resultant electrostatic force upon a dipole. The attracting and repelling forces upon the opposite charges of the dipole are (Figure 3):

$$\vec{F} = \vec{E}q; \qquad \vec{E} = \frac{U}{r\ln\frac{r_o}{r_i}}\hat{\boldsymbol{r}}; \qquad \vec{F}_+ = \frac{Uq}{\left(r+\frac{d}{2}\right)\ln\frac{r_o}{r_i}}\hat{\boldsymbol{r}}; \qquad \vec{F}_- = -\frac{Uq}{\left(r-\frac{d}{2}\right)\ln\frac{r_o}{r_i}}\hat{\boldsymbol{r}}$$

The resultant force upon the dipole is:

$$\vec{F}_p = \vec{F}_+ + \vec{F}_- = \frac{Uq}{\ln\frac{r_o}{r_i}}\left[\frac{1}{r+\frac{d}{2}} - \frac{1}{r-\frac{d}{2}}\right]\hat{\boldsymbol{r}} = \frac{Uq}{\ln\frac{r_o}{r_i}}\left[\frac{2}{2r+d} - \frac{2}{2r-d}\right]\hat{\boldsymbol{r}}$$

$$\vec{F}_p = \frac{Uq}{\ln\frac{r_o}{r_i}}\left[\frac{4r-2d-4r-2d}{(2r+d)(2r-d)}\right]\hat{\boldsymbol{r}} = \frac{Uq}{\ln\frac{r_o}{r_i}}\left[\frac{-4d}{4r^2-d^2}\right]\hat{\boldsymbol{r}}$$

Since $d \ll r$, the d^2 term can be neglected:

$$\vec{F}_p = -\frac{Uqd}{r^2\ln\frac{r_o}{r_i}}\hat{\boldsymbol{r}}$$

By substituting the definition of an electric dipole $\vec{p} = q\vec{d}$, we obtain the resultant dielectrophoretic force on an elementary dipole:

$$\vec{F}_p = -\frac{Up}{r^2\ln\frac{r_o}{r_i}}\hat{\boldsymbol{r}}$$

The dielectrophoretic volume force density in the cylindrical capacitor is obtained by multiplying this force with the dipole volume density N_p:

$$\vec{f}_d = N_p\vec{F}_p = -\frac{UP}{r^2\ln\frac{r_o}{r_i}}\hat{\boldsymbol{r}} = -\frac{\left(\varepsilon-\varepsilon_0\right)UE}{r^2\ln\frac{r_o}{r_i}}\hat{\boldsymbol{r}}$$

$$\boxed{\vec{f}_d = -\frac{\left(\varepsilon-\varepsilon_0\right)U^2}{r^3\left(\ln\frac{r_o}{r_i}\right)^2}\hat{\boldsymbol{r}}} \tag{4}$$

The dielectrophoretic force upon an infinitesimal volume of dielectric is:

$$dV = lrd\theta\,dr; \qquad d\vec{F} = \vec{f}_d dV = -\frac{\left(\varepsilon-\varepsilon_0\right)U^2dV}{r^3\left(\ln\frac{r_o}{r_i}\right)^2}\hat{\boldsymbol{r}}$$

$$d\vec{F} = -\frac{\left(\varepsilon-\varepsilon_0\right)U^2lrd\theta\,dr}{r^3\left(\ln\frac{r_o}{r_i}\right)^2}\hat{\boldsymbol{r}} = -\frac{\left(\varepsilon-\varepsilon_0\right)U^2ld\theta\,dr}{r^2\left(\ln\frac{r_o}{r_i}\right)^2}\hat{\boldsymbol{r}}$$

The y component of this force (see Figure 3) is $dF_y = dF\sin\theta$. Integrating these infinitesimal forces over the whole volume of top dielectric we get the resultant dielectrophoretic force on the top half of capacitor $\vec{F}_{d1}$:

$$dF_y = -\frac{(\varepsilon_1 - \varepsilon_0)\, U^2 l}{r^2 \left(\ln \frac{r_o}{r_i}\right)^2} \sin\theta d\theta\, dr; \qquad K = -\frac{(\varepsilon_1 - \varepsilon_0)\, U^2 l}{\left(\ln \frac{r_o}{r_i}\right)^2}$$

$$F_y = K \int_{r_i}^{r_o} \int_0^{\pi} \frac{\sin\theta}{r^2} d\theta\, dr = K \int_{r_i}^{r_o} \frac{1}{r^2} \int_0^{\pi} \sin\theta d\theta\, dr = K \int_{r_i}^{r_o} \frac{1}{r^2} \left[-\cos\theta\right]_0^{\pi} dr = 2K \left[-\frac{1}{r}\right]_{r_i}^{r_o}$$

$$F_y = 2K \left(\frac{1}{r_i} - \frac{1}{r_o}\right) = \frac{2K\,(r_o - r_i)}{r_i r_o}$$

$$\boxed{\vec{F}_{d1} = -\frac{2\,(\varepsilon_1 - \varepsilon_0)\,(r_o - r_i)\, U^2 l}{r_i r_o \left(\ln \frac{r_o}{r_i}\right)^2} \hat{\boldsymbol{y}}} \tag{5}$$

The x force components were not calculated because they are symmetric to the y axis and cancel one another. Therefore, the resultant force has got only a y component.

2.2.3 Resultant Thrust on the Capacitor

Now that we have the equations for both, the electrostatic pressure force component (3), and also for the dielectrophoretic force component (5), the total resultant force on the capacitor can be calculated as the sum of these components Figure 1:

$$\vec{F}_r = \vec{F}_s + \vec{F}_d; \qquad \vec{F}_s = \vec{F}_{s1} + \vec{F}_{s2}; \qquad \vec{F}_d = \vec{F}_{d1} + \vec{F}_{d2}$$

$$\vec{F}_s = \frac{\varepsilon_1\,(r_o - r_i)\, U^2 l}{r_i r_o \left(\ln \frac{r_o}{r_i}\right)^2} \hat{\boldsymbol{y}} - \frac{\varepsilon_2\,(r_o - r_i)\, U^2 l}{r_i r_o \left(\ln \frac{r_o}{r_i}\right)^2} \hat{\boldsymbol{y}}$$

$$\vec{F}_s = -\frac{(\varepsilon_2 - \varepsilon_1)\,(r_o - r_i)\, U^2 l}{r_i r_o \left(\ln \frac{r_o}{r_i}\right)^2} \hat{\boldsymbol{y}} \tag{6}$$

$$\vec{F}_d = -\frac{2\,(\varepsilon_1 - \varepsilon_0)\,(r_o - r_i)\, U^2 l}{r_i r_o \left(\ln \frac{r_o}{r_i}\right)^2} \hat{\boldsymbol{y}} + \frac{2\,(\varepsilon_2 - \varepsilon_0)\,(r_o - r_i)\, U^2 l}{r_i r_o \left(\ln \frac{r_o}{r_i}\right)^2} \hat{\boldsymbol{y}}$$

$$\vec{F}_d = \frac{2\,(\varepsilon_2 - \varepsilon_1)\,(r_o - r_i)\, U^2 l}{r_i r_o \left(\ln \frac{r_o}{r_i}\right)^2} \hat{\boldsymbol{y}} \tag{7}$$

$$\boxed{\vec{F}_r = \frac{(\varepsilon_2 - \varepsilon_1)\,(r_o - r_i)\, U^2 l}{r_i r_o \left(\ln \frac{r_o}{r_i}\right)^2} \hat{\boldsymbol{y}}} \tag{8}$$

According to this equation (8) if the permittivities of the two dielectrics are different, then a non-zero reactionless thrust is predicted on the charged capacitor, pointing either in positive or negative y direction, depending on the permittivity values. The thrust pushes the capacitor towards the dielectric of lower permittivity. This is an unexpected result that violates Newton's 3rd law, and naturally we should be looking for errors in the derivation of this equation. In lack of mathematical errors, let's double check the validity of the basic equations that were used as a starting point in our calculations, and calculate the thrust using other methods as well.

2.3 Verifying the Basic Equations and Employing Alternative Methods

2.3.1 E-field Distribution

The validity of the axisymmetric distribution of the E-field and the expression for its intensity (1) in the capacitor can be verified by simulating the geometry in any FEM software that can solve the equation of electric Gauss' law $\nabla \cdot \vec{D} = \varrho$, using the correlation between E-field and the electric potential field $\vec{E} = -\nabla V$ (COMSOL, FEniCS, Elmer, etc.). This was performed, and confirmed to be correct.

2.3.2 Electrostatic Pressure

The starting equation for the calculation of electrostatic pressure force components was the $f = \frac{\sigma^2}{2\varepsilon}$. This can be found in standard textbooks of electromagnetics, and its validity can be confirmed using the law of energy conservation.

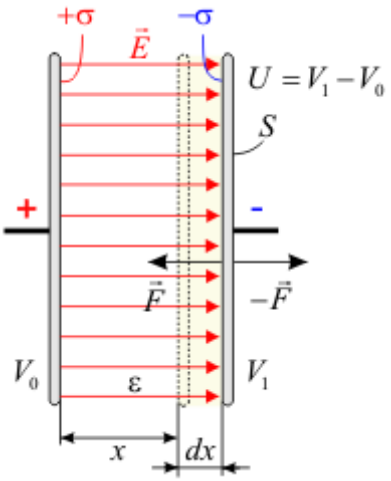

Figure 4: Deriving the equation of the electrostatic pressure from the law of energy conservation.

Let's derive the surface force density equation from the energy correlations of a parallel plate capacitor filled with a dielectric of permittivity ε, having a constant electric charge Q. For this theoretical calculation we assume that the distance between the plates x is much smaller than the size of the plates, therefore the edge effects can be neglected. A slightly compressible dielectric should be contained only in the regions where the E-field can be considered approximately homogeneous. This analysis will consider only that part of the capacitor which is filled with the dielectric, containing only the homogeneous part of the E-field. Despite the compressibility of the dielectric, it should have negligibly small electrostrictive coefficient, or the displacement dx should be small enough that the permittivity can be considered constant.

There is an attractive force between the electrodes, and if we increase the gap x between the plates by an infinitesimally small distance dx, then we have to perform a work of $-Fdx$ (Figure 4). According to the law of energy conservation this invested mechanical work will increase the electrical energy stored in the capacitor by $dW = Fdx$. From this correlation the attractive electric force can be calculated as:

$$\vec{F} = -\frac{dW}{dx}\hat{\boldsymbol{x}}; \qquad W = \frac{QU}{2} = \frac{Q^2}{2C}; \qquad C = \frac{\varepsilon S}{x}$$

$$W = \frac{Q^2 x}{2\varepsilon S}; \qquad \frac{dW}{dx} = \frac{Q^2}{2\varepsilon S}$$

$$\vec{F} = -\frac{Q^2}{2\varepsilon S}\hat{\boldsymbol{x}}$$

The force density on the surface of an electrode is $f = F/S$, from which follows the basic equation of electrostatic pressure on a perfect conductor surface ($\vec{n}$ - surface normal vector):

$$\vec{f} = \frac{Q^2}{2\varepsilon S^2}\vec{n}; \qquad \sigma = \frac{Q}{S}; \qquad \rightarrow \qquad \boxed{\vec{f} = \frac{\sigma^2}{2\varepsilon}\vec{n}}$$

This confirms that as long as the basic assumption of this derivation, the law of energy conservation is valid, this fundamental equation must be also valid. Therefore, we have good reason to accept the equation of the resultant electrostatic pressure force on the electrode surfaces of the cylindrical capacitor's top sector (3) as correct.

2.3.3 Dielectrophoretic Forces - Second Derivation Based on Kelvin Polarization Force Density

Our calculation of dielectrophoretic force component was based on electric forces acting upon the elementary charges of a molecular dipole, using the most basic definition of electric force $\vec{F} = q\vec{E}$. If there is anything

wrong with the implementation of this equation, then one place to look for it is in the interpretation of the electric field $\vec{E}$, which is assumed to be an external field; meaning that it excludes the field created by the test charge q. Although such an assumption seems to be trivial, there is a controversy about this subject researched by several authors like Frisch M. [1], Belot, G. [2], etc. Instead of getting into philosophical discussions about the validity or applicability of this basic definition, let's derive the dielectrophoretic force component in our capacitor via another method instead, and see if the result is the same as above.

The volume force that acts on the bulk of an electrically neutral dielectric in inhomogeneous E-field is also called Kelvin polarization force density:

$$\vec{f}_K = \vec{P} \cdot \nabla \vec{E} \tag{9}$$

This formula was nicely derived from the electric forces upon a dipole in *"Electromagnetic Fields and Energy"* MIT textbook [3]. That derivation is basically equivalent to our original calculation of dielectrophoretic component (both are based on electric forces on an elementary dipole), and we expect identical result as well.

In our case (and generally in most cases) $\vec{P}$ is an induced dipole moment density that is proportional to the E-field intensity $\vec{P} = (\varepsilon - \varepsilon_0)\,\vec{E}$, and the Kelvin force density from equation (9) takes the form of:

$$\vec{f}_K = \vec{P} \cdot \nabla \vec{E} = (\varepsilon - \varepsilon_0)\vec{E} \cdot \nabla \vec{E}$$

Using $\nabla \times \vec{E} = 0$ and [2] vector identities, the expression becomes:

$$\boxed{\vec{f}_K = \frac{1}{2}(\varepsilon - \varepsilon_0)\nabla(E^2)} \tag{10}$$

By substituting equation (1) for the E-field intensity, we obtain the Kelvin force density in our capacitor:

$$\vec{f}_K = \frac{1}{2}(\varepsilon - \varepsilon_0)\frac{\partial E_r^2}{\partial r}\hat{\boldsymbol{r}} = \frac{1}{2}(\varepsilon - \varepsilon_0)\frac{\partial}{\partial r}\left[\frac{U^2}{r^2\left(\ln\frac{r_o}{r_i}\right)^2}\right]\hat{\boldsymbol{r}}$$

$$\vec{f}_K = \frac{(\varepsilon - \varepsilon_0)U^2}{2\left(\ln\frac{r_o}{r_i}\right)^2}\frac{\partial}{\partial r}\left(\frac{1}{r^2}\right)\hat{\boldsymbol{r}}$$

$$\boxed{\vec{f}_K = -\frac{(\varepsilon - \varepsilon_0)U^2}{r^3\left(\ln\frac{r_o}{r_i}\right)^2}\hat{\boldsymbol{r}}} \tag{11}$$

This equation (11) is identical with the originally derived equation for the dielectrophoretic volume force density (4), therefore this calculation method leads to the same final result and reactionless thrust as the first calculation method. It supports the correctness of the first calculation, assuming that the basic equations of electrostatics are consistent, but it doesn't resolve the problem of Newton's 3rd law violation.

2.3.4 Calculating the Electric Forces From Maxwell Stress Tensor

As a third attempt to resolve the issue, let's see what insights can we gain about the total thrust on the capacitor, and about the force components within it based on Maxwell stress tensor $\mathbb{T}$. It is the most abstract of all relevant methods, because it doesn't differentiate between the force components of different origin. It lumps all force components together, and only the total resultant force on the examined volume can be calculated with it. There are two ways of calculating the total force on a body using the stress tensor.

1. The first method is to calculate the body force density within the volume as $\vec{f}_V = \nabla \cdot \mathbb{T}$, and integrate it over the whole volume $\vec{F}_V = \int_V \nabla \cdot \mathbb{T}\, dV$.

2. According to the second method, the surface force density $\vec{f}_S = \mathbb{T} \cdot \vec{n}$ is calculated, and integrated over the closed surface surrounding the volume $\vec{F}_S = \oint_S \mathbb{T} \cdot \vec{n}\, dS$.

Based on Gauss theorem, both approaches supposed to stand on their own and give identical results. The trivial application of the second method applied to a closed surface outside the dielectrics (completely enclosing both of them) gives a correct result of zero thrust for the whole capacitor, because the external E-field is assumed to be zero outside the dielectrics. But this trivial solution doesn't say anything about the internal

[2] $\vec{A} \cdot \nabla \vec{A} = (\nabla \times \vec{A}) \times \vec{A} + \frac{1}{2}\nabla(\vec{A} \cdot \vec{A})$

force components, and thus not really convincing and useful. If we want to gain insight into the force distribution within the capacitor, then we have to apply both methods on selected sub-volumes, and sub-surfaces, add the force components, and see if it still gives a zero total thrust like the trivial solution, according to the general expectations.

First Method: Integrating the Volume Force Density Let's find out what force components are predicted by the first approach on the two different dielectric sectors separately. First we derive the equation for the electric volume force density from the Maxwell stress tensor $\mathbb{T}$. The tensor is coordinate system independent, and it takes the following form in cylindrical coordinates in our capacitor (δ_{ij} - Kronecker delta):

$$E_\theta = 0; \qquad E_z = 0$$

$$\mathbb{T}_{ij} = \varepsilon \left(E_i E_j - \frac{1}{2} \delta_{ij} E^2 \right)$$

$$\mathbb{T} = \begin{bmatrix} \frac{1}{2}\varepsilon E_r^2 & 0 & 0 \\ 0 & -\frac{1}{2}\varepsilon E_r^2 & 0 \\ 0 & 0 & -\frac{1}{2}\varepsilon E_r^2 \end{bmatrix}$$

$$f_V = \nabla \cdot \mathbb{T} = \begin{bmatrix} \frac{\partial T_{rr}}{\partial r} + \frac{1}{r}\left[\frac{\partial T_{\theta r}}{\partial \theta} + (T_{rr} - T_{\theta\theta})\right] + \frac{\partial T_{zr}}{\partial z} \\ \frac{\partial T_{r\theta}}{\partial r} + \frac{1}{r}\left[\frac{\partial T_{\theta\theta}}{\partial \theta} + (T_{r\theta} + T_{\theta r})\right] + \frac{\partial T_{z\theta}}{\partial z} \\ \frac{\partial T_{rz}}{\partial r} + \frac{1}{r}\left[\frac{\partial T_{\theta z}}{\partial \theta} + T_{rz}\right] + \frac{\partial T_{zz}}{\partial z} \end{bmatrix} = \begin{bmatrix} \frac{1}{2}\varepsilon \frac{\partial E_r^2}{\partial r} + \frac{\varepsilon}{r} E_r^2 \\ 0 \\ 0 \end{bmatrix}$$

$$\vec{F}_V = \int_V \nabla \cdot \mathbb{T} \, dV$$

Excluding Electrode Boundaries If we calculate the force density excluding the sharp E-field gradient discontinuities at the electrode boundaries we get:

$$f_{Vr} = \frac{\varepsilon}{r} E_r^2 + \frac{\varepsilon}{2} \frac{\partial E_r^2}{\partial r} = \frac{\varepsilon U^2}{r^3 \left(\ln \frac{r_o}{r_i}\right)^2} + \frac{\varepsilon}{2} \frac{\partial}{\partial r} \frac{U^2}{r^2 \left(\ln \frac{r_o}{r_i}\right)^2} = \frac{\varepsilon U^2}{r^3 \left(\ln \frac{r_o}{r_i}\right)^2} + \frac{\varepsilon U^2}{2 \left(\ln \frac{r_o}{r_i}\right)^2} \frac{\partial}{\partial r} \frac{1}{r^2} = \frac{\varepsilon U^2}{r^3 \left(\ln \frac{r_o}{r_i}\right)^2} - \frac{\varepsilon U^2}{r^3 \left(\ln \frac{r_o}{r_i}\right)^2}$$

$$f_{Vr} = 0 \tag{12}$$

According to this result there is no electrical body force anywhere inside the dielectric independent of permittivity, therefore the total thrust on the dielectrics of capacitor $\vec{F}_{MVd}$ is also zero for any dielectric combination. For the correct interpretation of this result we should keep in mind that these calculations are based on E-field derivatives, which are not defined at E-field discontinuities, like at the boundary surfaces between dielectrics and electrodes. Therefore, this result is valid only for the case when the boundaries of the examined volume don't include the free and bound charges at the actual electrode boundaries.

Another point to consider is that even though the $f_{Vr} = \nabla \cdot \mathbb{T}$ is a theoretical volume force density, it does not correspond to a real physical body force density, like the ponderomotive Kelvin polarization force density. It is a purely mathematical quantity that includes the combined effects of all electric forces on the cut out volume, in our case both ponderomotive forces and also surface forces that act on the charges at the surface of the cut out volume of dielectric. The result of $f_{Vr} = 0$ conveys the meaning that if we cut out any volume from either dielectric in the capacitor (but leave it in place, with an infinitesimally thin gap between its surface and the surrounding dielectric mass), then the combined effect of real ponderomotive and surface forces will be zero, but it offers no insight into the values of these force components, nor does it clarify whether they exist at all. This solution is analogous to the trivial application of the second method applied to a closed surface outside the dielectrics, as mentioned above. We haven't gained any useful insight into the force components inside the capacitor, even though in this case the electrode boundaries were excluded from the calculation.

Including Electrode Boundaries Let's repeat the last calculation with the electrodes included in the test volume. In this case the E-field discontinuity at the electrode boundaries needs to be converted into a differentiable E-field domain. This can be done by theoretically expanding the electrode boundary surfaces into 3D, to have an infinitesimal thickness h, and assuming that the E-field intensity inside this layer is linearly changing from the local values in the dielectric to zero in the conductor.

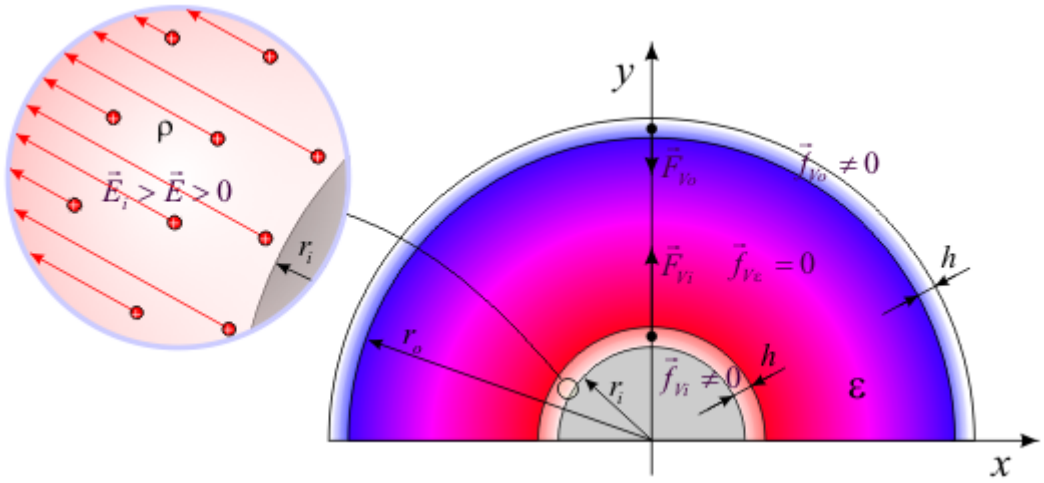

Figure 5: Converting the 2D electrode boundary surface into a 3D layer of thickness h.

First we calculate the unidirectional force on the top 180° sector of outer electrode boundary. With this transformation the E-field intensity inside this boundary layer is:

$$\vec{E} = \vec{E}_o \frac{h-(r-r_o)}{h}; \qquad r_o < r < r_o + h$$

$$f_{Vor} = \frac{\varepsilon}{r}E_r^2 + \frac{\varepsilon}{2}\frac{\partial E_r^2}{\partial r} = \frac{\varepsilon E_{or}^2}{rh^2}\left[h^2 - 2h\,(r-r_o) + (r-r_o)^2\right] + \frac{\varepsilon E_{or}^2}{2h^2}\frac{\partial}{\partial r}\left[h^2 - 2h\,(r-r_o) + (r-r_o)^2\right]$$

$$\Big/ \frac{\partial}{\partial r}\left[h^2 - 2h\,(r-r_o) + \left(r^2 - 2rr_o + r_o^2\right)\right] = -2h + 2r - 2r_o \Big/$$

$$f_{Vor} = \frac{\varepsilon E_{or}^2}{rh^2}\left[h^2 - 2h\,(r-r_o) + (r-r_o)^2\right] + \frac{\varepsilon E_{or}^2}{h^2}\left[r - r_o - h\right]$$

$$f_{Vor} = \frac{\varepsilon E_{or}^2}{rh^2}\left[h^2 - \underline{2hr} + 2hr_o + \overline{r^2} - \underbrace{2rr_o}_{} + r_o^2 + \overline{r^2} - \underbrace{rr_o}_{} - \underline{hr}\right]$$

$$f_{Vor} = \frac{\varepsilon E_{or}^2}{rh^2}\left[h^2 - 3hr + 2hr_o + 2r^2 - 3rr_o + r_o^2\right] = \frac{\varepsilon E_{or}^2}{rh^2}\left[2r^2 - 3hr - 3rr_o + \left(r_o^2 + 2hr_o + h^2\right)\right]$$

$$f_{Vor} = \frac{\varepsilon E_{or}^2}{rh^2}\left[2r^2 - 3r\,(r_o+h) + (r_o+h)^2\right]$$

Unlike in the previous case, the volume force is not zero in this thin layer. The radial force component dF_{Vor} on an infinitesimal volume dV is:

$$dV = lrd\theta\,dr \qquad dF_{Vor} = f_{Vor}dV = \frac{\varepsilon E_{or}^2 l}{h^2}\left[2r^2 - 3r\,(r_o+h) + (r_o+h)^2\right]d\theta\,dr$$

The Cartesian y component of this force is $dF_{Voy} = dF_{Vor}\sin\theta$. By integrating these force components over the layer volume we obtain the unidirectional force on it in vertical direction F_{Voy} (the x component cancels out):

$$dF_{Voy} = \frac{\varepsilon E_{or}^2 l}{h^2}\left[2r^2 - 3r\,(r_o+h) + (r_o+h)^2\right]\sin\theta\,d\theta\,dr; \qquad K = \frac{\varepsilon E_{or}^2 l}{h^2}$$

$$F_{Voy} = K \int_{r_o}^{r_o+h} \int_{0}^{\pi} \left[2r^2 - 3r\left(r_o + h\right) + \left(r_o + h\right)^2\right] \sin\theta \, d\theta \, dr = K \int_{r_o}^{r_o+h} \left[2r^2 - 3r\left(r_o + h\right) + \left(r_o + h\right)^2\right] \int_{0}^{\pi} \sin\theta \, d\theta \, dr$$

$$F_{Voy} = K \int_{r_o}^{r_o+h} \left[2r^2 - 3r\left(r_o + h\right) + \left(r_o + h\right)^2\right] \left[-\cos\varphi\right]_0^{\pi} \, dr = 2K \left[\frac{2r^3}{3} - \frac{3r^2\left(r_o + h\right)}{2} + r\left(r_o + h\right)^2\right]_{r_o}^{r_o+h}$$

$$F_{Voy} = 2K \left[\frac{4r^3 - 9r^2\left(r_o + h\right) + 6r\left(r_o + h\right)^2}{6}\right]_{r_o}^{r_o+h}$$

$$F_{Voy} = \frac{K}{3}\left[4\left(r_o + h\right)^3 - 9\left(r_o + h\right)^2\left(r_o + h\right) + 6\left(r_o + h\right)\left(r_o + h\right)^2 - 4r_o^3 + 9r_o^2\left(r_o + h\right) - 6r_o\left(r_o + h\right)^2\right]$$

$$F_{Voy} = \frac{K}{3}\left[\left(r_o^3 + 3hr_o^2 + 3h^2r_o + h^3\right) - 4r_o^3 + 9r_o^3 + 9hr_o^2 - 6r_o\left(r_o^2 + 2hr_o + h^2\right)\right]$$

$$F_{Voy} = \frac{K}{3}\left[\cancel{r_o^3} + \cancel{3hr_o^2} + \underline{3h^2r_o} + h^3 - \cancel{4r_o^3} + \cancel{9r_o^3} + \cancel{9hr_o^2} - \cancel{6r_o^3} - \cancel{12hr_o^2} - \underline{6h^2r_o}\right] = \frac{K}{3}\left[h^3 - 3h^2r_o\right]$$

$$F_{Voy} = \frac{Kh^2}{3}\left[h - 3r_o\right] = \frac{\varepsilon E_{or}^2 l}{3}\left[h - 3r_o\right]$$

Taking the layer thickness h to be much smaller than the outer radius $h \ll r_o$, the final form of this equation is:

$$F_{Voy} = -\varepsilon E_{or}^2 r_o l$$

Repeating the same calculation for the top inner boundary using a linear E-field transition of:

$$\vec{E} = \vec{E}_i \frac{(r - r_i)}{h}; \qquad r_i < r < r_i + h$$

we get the y force component on it:

$$F_{Viy} = \varepsilon E_{ir}^2 r_i l$$

The sum of these two opposing forces is the resultant vertical electric force on the top 180° sector (since according to (12) there is no force inside the dielectrics):

$$F_{V1y} = \varepsilon_1\left(E_{ir}^2 r_i - E_{or}^2 r_o\right) l = \frac{\varepsilon_1 U^2 l}{\left(\ln\frac{r_o}{r_i}\right)^2}\left(\frac{1}{r_i} - \frac{1}{r_o}\right)$$

$$\vec{F}_{V1} = \frac{\varepsilon_1\left(r_o - r_i\right)U^2 l}{r_i r_o\left(\ln\frac{r_o}{r_i}\right)^2}\hat{\boldsymbol{y}} \tag{13}$$

This is identical with equation (3) that represents the electrostatic pressure on the top 180° sector electrode surface caused by the surface charges. The total thrust on the capacitor according to this method (including the electrodes) is the sum of these components on the top and bottom halves (using the appropriate permittivity values) $\vec{F}_{MVe} = \vec{F}_{V1} + \vec{F}_{V2}$:

$$\boxed{\vec{F}_{MVe} = -\frac{\left(\varepsilon_2 - \varepsilon_1\right)\left(r_o - r_i\right)U^2 l}{r_i r_o\left(\ln\frac{r_o}{r_i}\right)^2}\hat{\boldsymbol{y}}} \tag{14}$$

which is identical with equation (6). It appears that the volume force integration method of the Maxwell stress tensor on the whole capacitor, including the electrode boundaries accurately predicts the effect of the electrostatic pressure on the electrodes, but ignores the presence of any ponderomotive force inside the dielectrics,

which is an incorrect result. It predicts a reactionless resultant thrust on the capacitor violating Newton's 3rd law, but the magnitude and direction of this thrust is not the same as predicted by the direct calculations, and by the method using Kelvin polarization force density.

One could argue that our first attempt to calculate the Maxwell volume forces as applied exclusively to the volume of dielectrics (excluding the electrode boundaries) has already predicted a correct zero total thrust, which agrees with Newton's 3rd law. Therefore, that should be the correct application method of the Maxwell stress tensor, and the calculations in the theoretically expanded boundary layer are entirely unphysical, unnecessary, and incorrect. However, it is quite possible to build such a capacitor as a physical device, that indeed has got a 3D layer of electrode boundary, filled with space charge, instead of the surface charge on conductors. If the electrode is made of a semiconductor with low doping concentration instead of metal, then it is possible to physically recreate our theoretical dielectric-electrode boundary of finite thickness, in which the E-field intensity gradually decreases to zero, having a well defined derivative. Therefore, our last approach should be correct for at least such a capacitor with semiconductor electrodes, still violating Newton's 3rd law.

Second Method: Integrating the Surface Force Density The second method that involves the calculation of a surface force density from the Maxwell stress tensor as $\vec{f}_S = \mathbb{T} \cdot \vec{n}$, and its integration over a closed test surface, inherently excludes the possibility of any resultant reactionless thrust on a body. This is because all sub-volumes (if we use more than one) must completely fill the examined body with their surfaces touching each other, and consequently all internal surface forces will mutually cancel one another. The total resultant force on the test surface containing the examined body is exclusively determined by the E-field (and surface forces) on its external surface; which in turn must be opposed by the reaction forces from the environment, if there is any external E-field. If there is no E-field on the external surface, then this method will predict a trivially zero resultant electric force on it, just like in our case.

This method allows us to calculate the resultant force not only upon macroscopic volumes, but also on infinitesimally thin boundary surfaces (like the electrode surfaces) with relative ease, without having to transform the surface into a 3D layer with smooth E-field gradients. The resultant electric force on a volume within a closed test surface S is calculated as:

$$\vec{F}_S = \oint_S \mathbb{T} \cdot \vec{n}\, dS$$

It was already mentioned that the most straightforward and trivial application of this method to our capacitor is to calculate the total force on a closed test surface that completely encloses the whole capacitor, having the surfaces of the test volume outside of the outer electrode. In this case the E-field intensity is zero everywhere on the test surface, which means that the surface force density is also zero everywhere, therefore the resultant thrust on the capacitor will be zero as well.

But we would like to gain at least some insight into what force components are predicted by this model inside the capacitor. Let's break up the geometry into 8 sub volumes, each contained by closed test surfaces, and see how the internal surface forces cancel one another, while comparing the forces on sub volumes to earlier derived expressions.

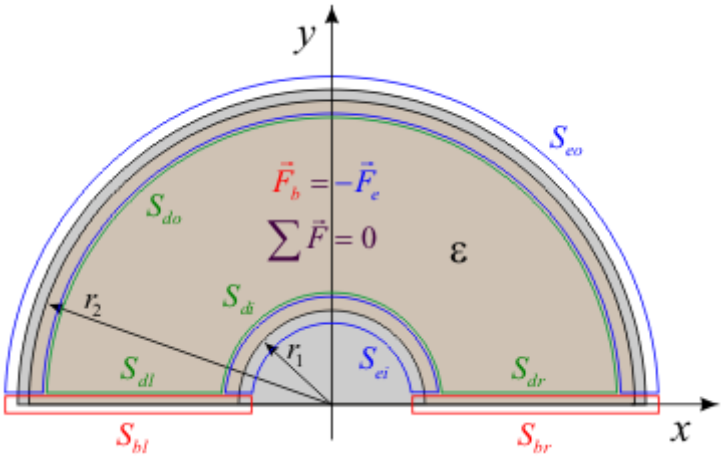

Figure 6: Sub volumes for surface force density integration (thickness exaggerated).

Surface Force Density on the Electrodes Lets calculate first the surface force density on the top 180° sector of the outer electrode. This semi-cylindrical segment of the electrode is enclosed by a test surface (outer blue lines on Figure 6) that is parallel to the electrode surface both inside and outside, and it cuts trough the electrode along the x axis with two horizontal flat plane surfaces. There is no E-field on the flat surfaces inside the conductor, nor on the external surface, therefore no surface force can act on these test surface segments, and we can ignore them. Only the internal surface segment within the dielectric needs to be analyzed.

The normal vector to this surface is $\vec{n} = (-1, 0, 0)$, and the electric surface force density on it is:

$$\vec{f}_{Seo1} = \mathbb{T} \cdot \vec{n} = \begin{bmatrix} \frac{1}{2}\varepsilon_1 E_{r_o}^2 & 0 & 0 \\ 0 & -\frac{1}{2}\varepsilon_1 E_{r_o}^2 & 0 \\ 0 & 0 & -\frac{1}{2}\varepsilon_1 E_{r_o}^2 \end{bmatrix} \begin{bmatrix} -1 \\ 0 \\ 0 \end{bmatrix} = \begin{bmatrix} -\frac{1}{2}\varepsilon_1 E_{r_o}^2 \\ 0 \\ 0 \end{bmatrix} = -\frac{1}{2}\varepsilon_1 E_{r_o}^2 \hat{\boldsymbol{r}}$$

The electrostatic pressure on the surface of a conductor is $f_S = \frac{\sigma^2}{2\varepsilon} = \frac{\varepsilon E^2}{2}$, which is identical with the obtained result. Therefore, we can conclude that in this particular case the model has accurately predicted the magnitude of the electrostatic pressure on the electrode surface, which is a real physical surface force density.

If we repeat this calculation for the top half of the inner electrode, then again only the top segment of the closed test surface in the dielectric needs to be analyzed, because there is no E-field inside the conductor or outside the dielectrics. In this case the normal vector to the test surface is $\vec{n} = (1, 0, 0)$, and the surface force density is:

$$\vec{f}_{Sei1} = \frac{1}{2}\varepsilon_1 E_{r_i}^2 \hat{\boldsymbol{r}}$$

The integration of these surface force densities over the top 180° sector was already performed in 2.2.1 and their sum (for the inner and outer electrodes) is the equation (3), therefore we can reuse that formula here as well:

$$\boxed{\vec{F}_{Se1} = \frac{\varepsilon_1 (r_o - r_i) U^2 l}{r_i r_o \left(\ln \frac{r_o}{r_i}\right)^2} \hat{\boldsymbol{y}}} \tag{15}$$

Surface Force Density on Dielectrics These closed test surfaces surround each dielectric completely, but exclude the electrode boundaries, and the boundary surface between the two dielectrics (green lines on Figure 6). The test surface that surrounds the top dielectric is made of a semi-cylinder of radius r_o, another semi-cylinder of radius r_i, and two radial plane surfaces on the right and left side of the inner electrode. The normal vector to the test surface below the outer electrode is $\vec{n} = (1, 0, 0)$, and the surface force density on it is (the same as $-\vec{f}_{Seo1}$):

$$\vec{f}_{Sdo1} = \frac{1}{2}\varepsilon_1 E_{r_o}^2 \hat{\boldsymbol{r}}$$

The normal vector to the test surface just above the inner electrode is $\vec{n} = (-1, 0, 0)$, and the surface force density on it is (the same as $-\vec{f}_{Sei1}$):

$$\vec{f}_{Sdi1} = -\frac{1}{2}\varepsilon_1 E_{r_i}^2 \hat{\boldsymbol{r}}$$

Reusing the results of previous calculations the sum of forces on the inner and outer semi-cylindrical surfaces is the negative of (15):

$$\vec{F}_{Sdio1} = -\frac{\varepsilon_1 (r_o - r_i) U^2 l}{r_i r_o \left(\ln \frac{r_o}{r_i}\right)^2} \hat{\boldsymbol{y}} \tag{16}$$

The normal vector to the radial plane segment of the test surface just above the right boundary between the two dielectrics is $\vec{n} = (0, -1, 0)$, and the surface force density on it is:

$$\vec{f}_{Sdr1} = \frac{1}{2}\varepsilon_1 E_r^2 \hat{\boldsymbol{\theta}}; \qquad \theta = 0$$

Since the gap between this plane and the boundary between the two dielectrics is infinitesimally small, we can approximate this part of the test surface to be normal to the Cartesian y axis. This transformation will

allow us to directly calculate the unidirectional y component of the force that acts on this surface. The force density components on it in Cartesian system are $\vec{f}_{Sdr1} = (0, \frac{1}{2}\varepsilon_1 E_r^2, 0)$. By integrating the y component over this plane surface we get the total force on it:

$$F_{Sdr1y} = \int_S f_{Sdr1} dS = \int_{r_i}^{r_o} \frac{\varepsilon_1}{2} E_r^2 l dr = \int_{r_i}^{r_o} \frac{\varepsilon_1 U^2 l}{2r^2 \left(\ln \frac{r_o}{r_i}\right)^2} dr = \frac{\varepsilon_1 U^2 l}{2\left(\ln \frac{r_o}{r_i}\right)^2} \int_{r_i}^{r_o} \frac{1}{r^2} dr$$

$$F_{Sdr1y} = \frac{\varepsilon_1 U^2 l}{2\left(\ln \frac{r_o}{r_i}\right)^2} \left[-\frac{1}{r}\right]_{r_i}^{r_o} = \frac{\varepsilon_1 U^2 l}{2\left(\ln \frac{r_o}{r_i}\right)^2} \left(\frac{1}{r_i} - \frac{1}{r_o}\right) = \frac{\varepsilon_1 (r_o - r_i) U^2 l}{2 r_i r_o \left(\ln \frac{r_o}{r_i}\right)^2}$$

The normal vector to the radial plane segment of the test surface just above the left boundary between the two dielectrics is $\vec{n} = (0, 1, 0)$, and the surface force density on it is:

$$\vec{f}_{Sdl1} = -\frac{1}{2}\varepsilon_1 E_r^2 \hat{\boldsymbol{\theta}}; \qquad \theta = \pi$$

The force on it can be calculated similarly as for the right plane segment, yielding identical result. The total force on the bottom plane surface segments above the dielectric boundaries is the sum of the forces on the right and left:

$$\vec{F}_{Sdlr1} = \frac{\varepsilon_1 (r_o - r_i) U^2 l}{r_i r_o \left(\ln \frac{r_o}{r_i}\right)^2} \hat{\boldsymbol{y}} \tag{17}$$

The total resultant force upon the top dielectric volume enclosed by the test surface is the sum of (17) and (16):

$$\vec{F}_{Sd1} = \vec{F}_{Sdlr1} + \vec{F}_{Sdio1} = \frac{\varepsilon_1 (r_o - r_i) U^2 l}{r_i r_o \left(\ln \frac{r_o}{r_i}\right)^2} \hat{\boldsymbol{y}} - \frac{\varepsilon_1 (r_o - r_i) U^2 l}{r_i r_o \left(\ln \frac{r_o}{r_i}\right)^2} \hat{\boldsymbol{y}}$$

$$\boxed{\vec{F}_{Sd1} = 0} \tag{18}$$

This is a noteworthy result, which can be interpreted in two different ways. The trivial interpretation is that there are no dielectrophoretic volume forces in the dielectric, and no electrostatic pressure on the test surface either, which is apparently incorrect. The second interpretation is that the dielectrophoretic volume forces of the first dielectric plus whatever force originates from the bottom half of the capacitor through the dielectric boundary exactly cancel the electrostatic pressure forces. Unfortunately it is not possible to separate only the dielectrophoretic forces from (17).

Total Force on the Boundary Between Dielectrics The boundary surfaces between the two dielectrics have to be analyzed separately, because according to this model imaginary forces can exist on these surfaces, which don't correspond to real physical forces present at these surfaces. It is standard practice for the calculation of dielectrophoretic pressure in the Pellat's experiment to integrate the Maxwell stress on the closed test surface that surrounds the liquid-air boundary. This method has also accurately predicted the electrostatic pressure on the electrodes (15).

If we integrate the Maxwell surface forces on both electrode sectors (top & bottom) based on (15), we get the equivalent of (6) that represents the real electrostatic pressure component on the electrodes:

$$\vec{F}_{Se} = -\frac{(\varepsilon_2 - \varepsilon_1)(r_o - r_i) U^2 l}{r_i r_o \left(\ln \frac{r_o}{r_i}\right)^2} \hat{\boldsymbol{y}} \tag{19}$$

In this case there are no unknown forces originating from the other sector, but the only remaining force components are on the boundaries between the two dielectrics. Therefore, we can reasonably expect that the forces calculated on the dielectric boundaries would also represent the dielectrophoretic body forces (like in Pellat's experiment), even though the location and real physical nature of the predicted forces are incorrect.

Let's integrate the Maxwell surface force density on the closed test surface surrounding the right boundary between the two dielectrics. The test surface is composed of one radial flat plane just above the boundary, another similar plane just below the boundary, one cylindrical surface segment at the outer electrode, and another similar surface at the inner electrode (right red line on Figure 6). Since the tiny cylindrical segments on the right and left are outside the dielectrics where there is no E-field, they can be ignored.

The normal vector to the top radial plane component of the test surface is $\vec{n} = (0, 1, 0)$, and the surface force density on it is:

$$\vec{f}_{Sbr1} = -\frac{1}{2}\varepsilon_1 E_r^2 \hat{\boldsymbol{\theta}}; \qquad \theta = 0$$

Repeating the same calculation for the bottom component of the test surface located in the second dielectric using the normal vector $\vec{n} = (0, -1, 0)$ we get:

$$\vec{f}_{Sbr2} = \frac{1}{2}\varepsilon_2 E_r^2 \hat{\boldsymbol{\theta}}; \qquad \theta = 0$$

The angle θ between the two radial surfaces are infinitesimally small, therefore we can approximate them to be parallel, and normal to the Cartesian y axis. This transformation will allow us to directly calculate the unidirectional y component of the force that acts on the boundary. The sum of these opposing force density components now in Cartesian system is $\vec{f}_{Sbr} = (0, \frac{1}{2}(\varepsilon_2 - \varepsilon_1)E_r^2, 0)$. By integrating the y component of this over the boundary we get the total force on it:

$$F_{Sbry} = \int_S f_{Sbr} dS = \int_{r_i}^{r_o} \frac{(\varepsilon_2 - \varepsilon_1)}{2} E_r^2 l \, dr = \int_{r_i}^{r_o} \frac{(\varepsilon_2 - \varepsilon_1)U^2 l}{2r^2 \left(\ln \frac{r_o}{r_i}\right)^2} dr = \frac{(\varepsilon_2 - \varepsilon_1)U^2 l}{2\left(\ln \frac{r_o}{r_i}\right)^2} \int_{r_i}^{r_o} \frac{1}{r^2} dr$$

$$F_{Sbry} = \frac{(\varepsilon_2 - \varepsilon_1)U^2 l}{2\left(\ln \frac{r_o}{r_i}\right)^2} \left[-\frac{1}{r}\right]_{r_i}^{r_o} = \frac{(\varepsilon_2 - \varepsilon_1)U^2 l}{2\left(\ln \frac{r_o}{r_i}\right)^2} \left(\frac{1}{r_i} - \frac{1}{r_o}\right) = \frac{(\varepsilon_2 - \varepsilon_1)(r_o - r_i)U^2 l}{2 r_i r_o \left(\ln \frac{r_o}{r_i}\right)^2}$$

The force on the left boundary can be calculated similarly. The total force on the dielectric boundaries is the sum of the forces on the right and left:

$$\boxed{\vec{F}_{MSb} = \frac{(\varepsilon_2 - \varepsilon_1)(r_o - r_i)U^2 l}{r_i r_o \left(\ln \frac{r_o}{r_i}\right)^2} \hat{\boldsymbol{y}}} \tag{20}$$

This result is the exact opposite of the electrostatic pressure force on the electrodes represented by equation (19), and they cancel one another. There are only two types of electric forces in the capacitor, and the electrostatic pressure type was already accurately calculated. It follows then that equation (20) must represent the sum of dielectrophoretic forces in both dielectrics. If we take the last equation (20) to represent the dielectrophoretic forces (even though the location is incorrect), then its magnitude satisfies Newton's 3rd law.

2.3.5 Dielectrophoretic Forces - Fourth Derivation From the Korteweg-Helmholtz Equation

The dielectrophoretic forces in our capacitor can be also calculated using the Korteweg–Helmholtz electric force density equation (21) (ϱ - space charge density; ρ - mass density of the medium), which was derived from the energy principles [9, 10, 11], and doesn't provide an accurate insight into the exact place and physical nature of the forces, but it has been accepted to accurately predict the total force on a finite volume of medium. Let's derive the dielectrophoretic force component in our cylindrical capacitor based on this equation.

$$\vec{f}_V = \varrho\vec{E} - \frac{1}{2}E^2\nabla\varepsilon + \frac{1}{2}\nabla\left(E^2\rho\frac{\partial\varepsilon}{\partial\rho}\right) \tag{21}$$

The first component is the force acting on free space charge ϱ, which can be ignored in our case because all free charges are on the boundary surface of the electrodes, and their effect was calculated separately. The last component is caused by electrostriction when the medium is compressible, and the permittivity is the function of mass density. This is again zero, since we use ideal incompressible dielectrics.

Therefore only the second component needs to be taken into consideration, which is the force density component caused by permittivity gradients. It basically says that an electric body force density acts upon the medium in any volume where a permittivity gradient exists, which is proportional to the product of this gradient and the square of the E-field intensity. It is interesting to note that the direction of this force is determined only by the gradient, and it is independent of the direction of the E-field.

There are no smooth continuous permittivity gradients in our capacitor, but there is a sharp jump at the boundary surface between the two dielectrics. In order to make this abstract formulation applicable to our problem, we have to approximate this sharp permittivity discontinuity as a very thin 3D layer of thickness $h \to 0$

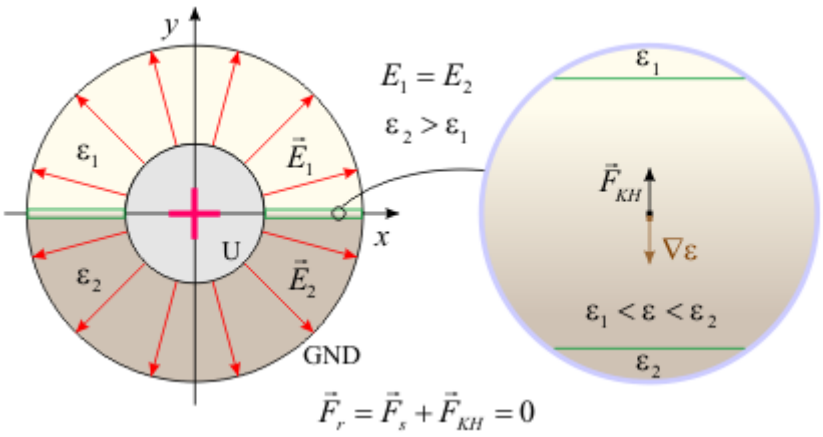

Figure 7: Boundary layer of finite thickness between the two dielectrics.

at the boundary surface, in which volume the permittivity linearly changes from ε_2 to ε_1 in y direction (a quadratic function of ε leads to the same result), thus it has got a finite permittivity gradient (Figure 7).

$$\varepsilon = \varepsilon_2 - y\frac{\varepsilon_2 - \varepsilon_1}{h}; \qquad 0 < y < h$$

$$\nabla\varepsilon = \frac{\partial\varepsilon}{\partial y}\hat{\boldsymbol{y}} = -\frac{\varepsilon_2 - \varepsilon_1}{h}\hat{\boldsymbol{y}}$$

$$\vec{f}_V = -\frac{1}{2}E^2\nabla\varepsilon = E^2\,\frac{\varepsilon_2 - \varepsilon_1}{2h}\hat{\boldsymbol{y}}$$

There are two boundary surfaces between the two dielectrics, therefore we multiply the integrated force by 2:

$$\vec{F}_{KH} = 2\int_V \vec{f}_V\,dV = 2\int_{x=r_i}^{r_o}\int_{y=0}^{h} \vec{f}_V\,l\,dy\,dx$$

If h is infinitesimally small, then we can approximate $\vec{E}$ to be independent of y coordinate having only an x component within this layer:

$$\vec{F}_{KH} = 2l\int_{x=r_i}^{r_o}\int_{y=0}^{h} E_x^2\frac{\varepsilon_2 - \varepsilon_1}{2h}dy\,dx\,\hat{\boldsymbol{y}} = \frac{\varepsilon_2 - \varepsilon_1}{h}l\int_{x=r_i}^{r_o}\frac{U^2}{x^2\left(\ln\frac{r_o}{r_i}\right)^2}\int_{y=0}^{h} dy\,dx\,\hat{\boldsymbol{y}}$$

$$\vec{F}_{KH} = \frac{(\varepsilon_2 - \varepsilon_1)U^2 l}{\left(\ln\frac{r_o}{r_i}\right)^2}\int_{x=r_i}^{r_o}\frac{1}{x^2}dx\,\hat{\boldsymbol{y}} = \frac{(\varepsilon_2 - \varepsilon_1)U^2 l}{\left(\ln\frac{r_o}{r_i}\right)^2}\left[-\frac{1}{x}\right]_{r_i}^{r_o}\hat{\boldsymbol{y}} = \frac{(\varepsilon_2 - \varepsilon_1)U^2 l}{\left(\ln\frac{r_o}{r_i}\right)^2}\left(\frac{1}{r_i} - \frac{1}{r_o}\right)\hat{\boldsymbol{y}}$$

$$\boxed{\vec{F}_{KH} = \frac{(\varepsilon_2 - \varepsilon_1)(r_o - r_i)U^2 l}{r_i r_o\left(\ln\frac{r_o}{r_i}\right)^2}\hat{\boldsymbol{y}}} \tag{22}$$

This formula (22) represents the total ponderomotoric force component that is present within the capacitor, therefore it corresponds to the equation (7) (but it is only half of that value). In this case we have got a result that exactly cancels the electrostatic pressure component on the electrode surfaces (6), yielding zero total thrust on the capacitor. Thus, this method of calculating the dielectrophoretic force components satisfies Newton's 3rd law; there is no reactionless force predicted. We could rejoice now that the correct way of calculating the electrostatic forces on the capacitor was finally found; however, as much as it helped, that much it has also confused the situation.

The second term of Korteweg-Helmholtz equation predicts the presence of a vertical force component that is pushing the boundary layer between the two dielectrics in y direction towards the dielectric of lower permittivity. This is an unphysical prediction (despite the value of the calculated force being correct), because there are no free charges on this boundary surface, and there is no E-field component perpendicular to this surface. Therefore,

in physical reality no electric force can act on this boundary surface, as predicted by equation (22). Common practice is to ignore this lack of correspondence to physical reality, and accept it as normal. But a well developed, modern, and consistent EM theory should not contain such contradictions.

3 Experimental Verification

Since the above calculations based on classical EM theory led to contradictions, an experimental verification of the predicted reactionless thrust was carried out. The project was entirely financed by our own very limited private funds, therefore simple methods were employed, building and measuring everything ourselves. In order to assist the proper evaluation of our results, and prove the satisfactory accuracy of measurements, the building and experimental procedures will be described in sufficient detail to enable independent replications.

A coaxial cylindrical capacitor with two 180° sectors of different dielectrics was constructed according to Figure 1, and force measurements were performed on it. The expected thrust was measured with a sensitive torsion pendulum. The applied DC high voltage was provided by a 35kV HV PSU with continuously adjustable output voltage, and it was measured with a digital multimeter via a HV probe.

3.1 Construction of the Capacitor

The capacitor was made of two separable parts. One part was filled with polyester resin, holding the inner cylindrical electrode. The other part was a removable semi-cylindrical outer electrode. The outer electrode was made of two 15 cm long copper pipe sectors with 13 mm inner diameter and 1 mm wall thickness. We need two identical semi-cylinders both having exactly 180° arcs. The cutting wastes about 2 mm thick part of the pipe, therefore the two exactly 180° semi-cylinders were obtained from two 15 cm long pipes.

Figure 8: Parts of the coaxial cylindrical capacitor with two different dielectric sectors.

Four half-rings were made from 3 mm thick copper wires, and soldered to the ends of the semi-cylinders to obtain smooth, rounded edges that minimize the local E-field intensity, and prevent early sparking. After the

soldering, smooth joint surfaces were obtained by filing and sanding. An insulated wire was soldered to the middle of the second semi-cylinder to connect it to the voltage source (Figure 8).

The inner electrode was made of a 16 cm long aluminum pipe of 6 mm outer diameter. The soldering of aluminum is more difficult than that of copper, but by covering a piece of the 3 mm thick copper wire with thick solder in several layers, one can obtain a conductive plug that (after filing) fits tightly into the pipe's end. When the plug sits firmly in its place, more solder can be meted to it, and shaped into a hemispherical form with a file and sandpaper. At one end of the aluminum pipe an insulated wire was soldered into the middle of the hemispherical plug to connect it to the PSU.

A small plastic disc of 13 mm diameter with a 6 mm hole in its middle was cut into two halves. They were glued to the ends of the copper semi-cylinder with second glue. The aluminum electrode was then glued to this holder in similar way, and the assembly was filled with polyester resin. After the polyester hardened, the two plastic walls were removed and the resin surfaces cleaned, because uncured sticky paths appeared on the boundary surface between the resin and the plastic that could have caused early sparking. In the first measurement the other half of the coaxial capacitor has air as dielectric, thus the two semi-cylinders were placed upon each other, and fixed together with few turns of thin steel wire at both ends.

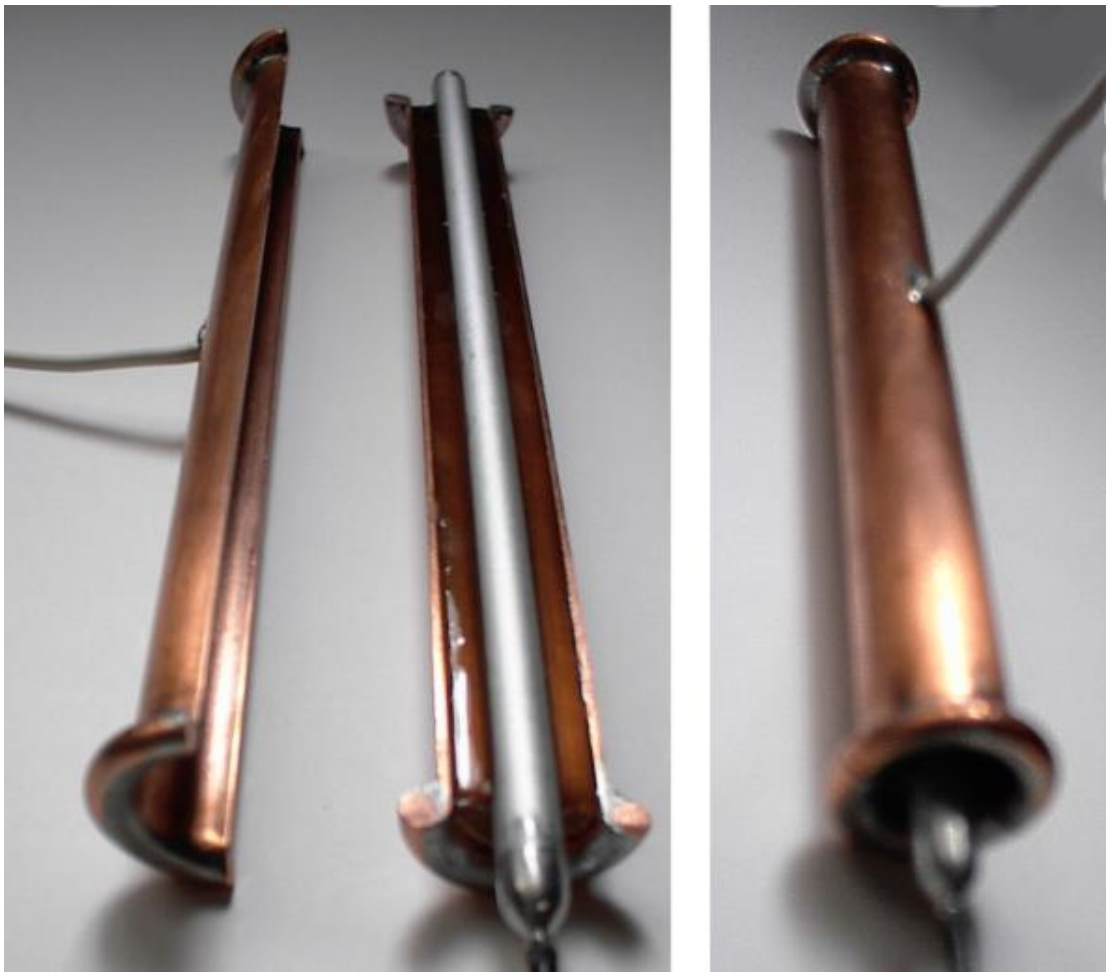

Figure 9: The finished 180° sector filled with polyester resin (left), and the assembled cylindrical capacitor (right).

3.2 Measuring the Relative Dielectric Constant of the Resin

The polyester resin had a relative dielectric constant of $\varepsilon_r = 6$, dielectric strength of 20 MV/m, volume resistivity of 10^{12} Ωm, and surface resistivity of 10^{13} Ω from the datasheet that was available at *www.kern-gmbh.de* around 2003. The $\varepsilon_r = 6$ was confirmed by measurements in the following way. The capacitance of a coaxial cylindrical capacitor with air dielectric is calculated with the formula:

$$C_0 = \frac{2\pi\varepsilon_0 l}{\ln\left(\frac{r_o}{r_i}\right)}$$

where: $\varepsilon_0 = 8.854 \cdot 10^{-12}$ As/Vm is the dielectric constant of vacuum; l – length of the capacitor; r_o – radius of the outer electrode; r_i – radius of the inner electrode. If we substitute l=0.153 m; r_i=3 mm; r_o=6.5 mm, then we get C_0=11 pF, and one half of the capacitor has got 5.5 pF capacitance. The capacitance of the assembled capacitor (one half polyester; the other air) was measured to be C=39 pF. This is made up by the sum of the two capacitances coupled in parallel, one having air as dielectric and thus having 5.5 pF capacitance, and the other is filled with polyester resin and having a capacitance of $5.5\,\varepsilon_r$ pF. The unknown relative dielectric constant of the resin can be calculated from the following equation: $5.5 + 5.5\,\varepsilon_r = 39$; $\varepsilon_r = (39 - 5.5)/5.5$; $\varepsilon_r = 6.1$. This is very close to the factory specified value of $\varepsilon_r = 6$.

3.3 Measuring the Expected Thrust

- **Polyester-air:**

The assembled capacitor with polyester and air as dielectrics was mounted on the beam of a sensitive torsion pendulum, making sure that the boundary surface between the dielectrics is oriented in radial direction, thus the expected thrust was oriented tangentially. After connecting it to the HV PSU, the applied voltage was slowly increased until sparking started between the electrodes at the ends of the capacitor at 7.5-8 kV.

No thrust could be detected within the $10^{-4} - 10^{-3}$ N range at this voltage, even though the expected thrust predicted by the formula (8) was $F_r = 0.13$ N. The predicted force is three orders of magnitude above the sensitivity of the torsion pendulum, therefore there would have been no difficulty with its detection.

The E-field intensity on the surface of the inner electrode calculated with equation (1) at $U = 8$ kV, when sparking occurs is about $E_i = 3.45$ MV/m, which is the same as the dielectric strength of the air, and this result is in good agreement with *Peek's* measurements [5]. Thus, the observed breakdown of the air started at the expected voltage.

- **Polyester-paraffin oil:**

In the next measurement both ends of the capacitor and the joints of the two semi-cylinders were sealed with bee's wax, but at the upper end two small openings were left in the wax plug. Paraffin oil was filled into the empty half of the capacitor through one hole (with a pipette), while the other hole was reserved for the air to escape.

Figure 10: The assembled capacitor sealed with bee's wax, ready to be filled with paraffin oil.

The relative dielectric constant of paraffin oil is $\varepsilon_r = 4.6 - 4.8$. The capacitor was mounted on the beam of the torsion pendulum and the voltage slowly increased until internal discharges were heard at the upper opening at about 20 kV. The dielectric strength of the oil supposed to allow much higher voltage without discharge, but there must have been some tiny air bubbles trapped at the top (below the wax plug), and this caused the early sparking. No thrust was detected in the $10^{-4} - 10^{-3}$ N range up till 20 kV using paraffin oil as the second dielectric, even though equation (8) predicted a reactionless thrust of $F_r = 0.119$ N at 15 kV and oil permittivity $\varepsilon_r = 4.8$.

4 Fitting the Equations to the Measured Facts

The measurement results confirmed the validity of Newton's 3rd law in the capacitor. Regardless of the dielectric constant of the dielectrics, and whether they are solid or liquid, no unidirectional reactionless thrust was

detected. However, they have also proven that some equations of classical EM theory, and/or the methods of calculating the resultant force on the capacitor don't model reality accurately.

The observed lack of resultant force on the capacitor could happen in two cases:

1. The first possibility could be that there is no unidirectional resultant thrust in either half of the coaxial cylindrical capacitor, because the electrostatic pressure forces cancel the dielectrophoretic forces in both halves independently. This option was disproved with further measurements.

2. The second possibility is that there are resultant unidirectional thrust components in both halves of the coaxial capacitor, but they have identical magnitudes and cancel each other. Since these thrust components are independent of the dielectrics, they must be the same as the thrust on one half of a cylindrical capacitor with vacuum between the electrodes. The measurements did confirm the validity of this theory, therefore let's change the equations so that they should describe this case, namely that the resultant thrust in one half of a cylindrical capacitor should be independent of the applied dielectric, being the same as in vacuum.

Comparing the formula of the electrostatic pressure force components (3), with the very similar formula of dielectrophoretic force components (5) in a 180° sector:

$$\vec{F}_s = \frac{\varepsilon\,(r_o - r_i)\,U^2 l}{r_i r_o \left(\ln \frac{r_o}{r_i}\right)^2}\hat{\boldsymbol{y}}; \qquad \vec{F}_d = -\frac{2\,(\varepsilon - \varepsilon_0)\,(r_o - r_i)\,U^2 l}{r_i r_o \left(\ln \frac{r_o}{r_i}\right)^2}\hat{\boldsymbol{y}}$$

it is obvious that if the number 2 would be eliminated from the equation of $\vec{F}_d$, then the sum of the two components would be independent of the dielectric constant of the filler dielectric ε (23), and the resultant thrust on the capacitor $\vec{F}_{rh}$ would become zero as expected and observed :

$$\vec{F}_{rh1} = \frac{\varepsilon_1\,(r_o - r_i)\,U^2 l}{r_i r_o \left(\ln \frac{r_o}{r_i}\right)^2}\hat{\boldsymbol{y}} - \frac{(\varepsilon_1 - \varepsilon_0)\,(r_o - r_i)\,U^2 l}{r_i r_o \left(\ln \frac{r_o}{r_i}\right)^2}\hat{\boldsymbol{y}}$$

$$\vec{F}_{rh1} = \frac{\varepsilon_0\,(r_o - r_i)\,U^2 l}{r_i r_o \left(\ln \frac{r_o}{r_i}\right)^2}\hat{\boldsymbol{y}} \tag{23}$$

$$\vec{F}_{rh} = \vec{F}_{rh1} - \vec{F}_{rh2} = 0$$

Equation (23) is the formula of the resultant unidirectional thrust on a 180° sector of cylindrical capacitor that is independent of the applied dielectric, and it is identical with the thrust in vacuum. The influence of the dielectric on the thrust is neutralized by the fact that as much as the electrostatic pressure force increases due to increased permittivity, the opposing dielectrophoretic force also increases equally. Consequently, it is not possible to establish thrust asymmetry in a coaxial cylindrical capacitor using two (or more) different homogeneous isotropic dielectrics. This is the only possible way to satisfy Newton's 3rd law, when the resultant forces ($\vec{F}_r = \vec{F}_s + \vec{F}_d$) upon both the upper and lower domains have identical magnitudes, pointing in opposite directions, as discussed earlier in section 2.1. This hypothetical version is also in agreement with the measurements.

Now that we have found the desired form of the equation for the dielectrophoretic force components, let's find out how we could derive this hypothetical form from basic principles, which is only half of the original $\vec{F}_d$. Since we have started our derivation of the dielectrophoretic forces based on the basic definition of $\vec{F} = \vec{E}q$ there is very little room for changes to fit the requirements. It was already mentioned that the E-field intensity must be axially symmetric and independent of the dielectric constant.

One possible modified hypothetical version of this definition would be $\vec{F}_h = \vec{E}\frac{q}{2}$ when the E-field intensity, and also the dipole moment density $\vec{P}$ would remain unchanged, but the electric force would act only upon half of the dipole's positive and negative charges. Even though this equation fitting would satisfy Newton's 3rd law in harmony with the measurements in this particular geometry, from physical point of view it doesn't make much sense at this point. It would also produce wrong results in geometries where the standard equation of the Kelvin polarization force density derived from $\vec{F} = \vec{E}q$ correctly predicts the dielectrophoretic forces as observed [12, 13].

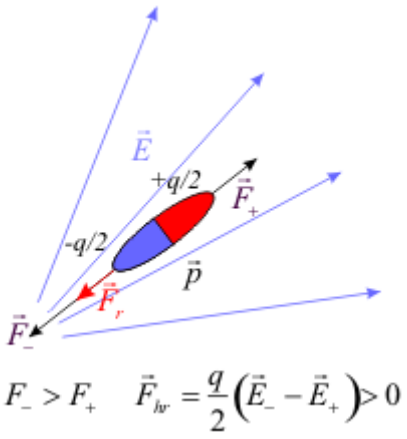

Figure 11: A possible modified model of the dielectrophoretic force upon an elementary dipole.

5 Summary

The starting point of presented calculations is the solution of the inhomogeneous E-field distribution within the capacitor, which is axially symmetrical, having only radial component, and independent of the dielectric constant. There are two different types of electric force components in our charged capacitor:

1. the electrostatic pressure, originating from free and bound surface charges at the electrodes,
2. the dielectrophoretic volume force (also called Kelvin force, L-DEP force, and ponderomotive force) in the bulk of dielectrics, originating from the asymmetrical electric forces on molecule dipoles in inhomogeneous E-fields.

In the above analysis we came to the conclusion that the derived equation of electrostatic pressure component must be correct, because any other variant would violate the law of energy conservation, and contradict accurate measurement results. Therefore in those cases where the calculations predicted the presence of a resultant reactionless force on the capacitor, we were looking for the error in the Kelvin force component.

Five different methods were employed for the calculation the dielectrophoretic force component, yielding different results. Table 1 summarizes the methods, derived results; evaluates their correctness and correspondence to real physical forces.

Calculation Method	Corresponding Dielectrophoretic Component Derived	Is the Magnitude Correct?	Are the Place and Physical Nature Correct?
Direct Method From $\vec{F} = \vec{E}q$ at Molecular Level	$\vec{F}_d = \frac{2(\varepsilon_2-\varepsilon_1)(r_o-r_i)U^2 l}{r_i r_o \left(\ln \frac{r_o}{r_i}\right)^2}\hat{\boldsymbol{y}}$	No	Yes
Kelvin Polarization Force Density $\vec{F}_K = \int_V \vec{P} \cdot \nabla \vec{E}\, dV$	$\vec{F}_K = \frac{2(\varepsilon_2-\varepsilon_1)(r_o-r_i)U^2 l}{r_i r_o \left(\ln \frac{r_o}{r_i}\right)^2}\hat{\boldsymbol{y}}$	No	Yes
Divergence of Maxwell Stress Tensor $\vec{F}_{MV} = \int_V \nabla \cdot \mathbb{T}\, dV$	$\vec{F}_{MVd} = 0$	No	N/A
Surface Force Density of Maxwell Stress Tensor $\vec{F}_{MS} = \oint_S \mathbb{T} \cdot \vec{n}\, dS$	$\vec{F}_{MSb} = \frac{(\varepsilon_2-\varepsilon_1)(r_o-r_i)U^2 l}{r_i r_o \left(\ln \frac{r_o}{r_i}\right)^2}\hat{\boldsymbol{y}}$	Yes	No
Korteweg-Helmholtz equation $\vec{F}_{KH} = -\int_V \frac{1}{2}\mathrm{E}^2 \nabla \varepsilon\, dV$	$\vec{F}_{KH} = \frac{(\varepsilon_2-\varepsilon_1)(r_o-r_i)U^2 l}{r_i r_o \left(\ln \frac{r_o}{r_i}\right)^2}\hat{\boldsymbol{y}}$	Yes	No

Table 1: Tabular summary of the dielectrophoretic force component calculation method results.

The fact that there are at least 5 different methods for the calculation of this component just reinforces the suspicion that our present model of dielectrophoresis might be incorrect or incomplete, and inconsistent

with the rest of the electromagnetic theory. For instance the Korteweg-Helmholtz equation offers a completely different expression for this force component than the expression of Kelvin polarization force density, which in itself is a red flag for the critical thinkers.

Another observation is that in the majority of scientific literature and related papers the authors make only cursory mention of Kelvin polarization force density formula, and prefer to use either the abstract Maxwell stress tensor, or the Korteweg-Helmholtz equation for the calculation of forces in their geometries. However, only the Kelvin force expression was derived from real microscopic physical forces, and only this formula places the action of the volume force density to the correct spot in the geometry. Only this expression explains the real physical action mechanism of this force component.

Why would anyone be motivated to use an abstract calculation method instead, which places the forces to the wrong place? The main argument for this practice was that the Kelvin force equation can be used only if the exact E-field distribution is known, which is not the case in most situations, because the geometry is complicated and it can't be resolved using analytic equations. This argument was quite convincing thus far, while the application of numerical methods were not sufficiently widespread, due to required expertise and expensive computer resources for its implementation. However, as cheap computing power and user-friendly FEM software become more and more accessible, an urgent need arises for the usage of Kelvin formula in these software models and simulations. Therefore, there is also an urgent need for the clarification of the confusion surrounding the ponderomotive forces at molecular scale.

The primary concern of this paper is to call the attention of professors of Electrical engineering, physicists, researchers, and anybody who is interested in the subject to contribute to the clarification of the presented issue of the direct method and the Kelvin polarization force density (which are essentially identical). As long as this problem is not satisfactorily resolved, the electromagnetic theory can not be considered consistent.

6 APPENDIX A: Claim of Priority

In an ideal world this section wouldn't be necessary, because people in general, especially scientists would be gentlemen enough to give credit where it is due. Unfortunately we don't live in an ideal world, and there have been already some attempts by people to take credit for the author's related work.

- Patent Sample

An awkward example is the British patent application GB2467114A "Reactionless electric-field thruster" filed on 2010-07-28, in which Terence Bates claims to be the inventor of the cylindrical/spherical capacitor with two (or more) segments of different dielectrics as a device generating reactionless thrust; the one that we have analyzed in this paper. His first related patent application GB0900122A "Reactionless electric field thruster" was submitted in 2009-01-06 but withdrawn. Apparently the patent GB0900122D0 "Reactionless electric field thruster" was granted to him on 2009-02-11, but the "Application withdrawn, taken to be withdrawn or refused ** after publication under section 16(1)" on 2014-10-15. These two last documents are inaccessible online, but the still ungranted GB2467114A can be downloaded by anyone.

First of all the device as a potential E-field thruster, and the discovery of the reactionless thrust prediction based on the presented scientific calculations was first published by the author of this paper in 2003 on his old website. Some of those pages are mirrored on another website, and still accessible to this day. The archive.org also carries the copies of those pages as proof. To this day I am not aware of anyone publishing this earlier. Mr. Bates is not the inventor of this device; it has been published in the public domain 6 years prior to his first patent application, and according to decent patent rules, inventions already in public domain can't be patented.

What makes this case really awkward, is the fact that we have also published the related measurements that disproved the presence of any thrust on the capacitor on our old website already in 2004. What sense does it make to patent a device that does not work in reality as claimed in the patent? If the applicant thought that our measurements were faulty, then he should have replicated them (or performed his own experiments) to see the truth for himself. If even non-functional inventions are plagiarized, just imagine what aggressive 'gold rush' and trampling would develop around such a discovery/invention if it would actually work, and generate reactionless thrust... However, to Mr. Bates' credit, at least he referred to this author's work in his latest patent application.

- Related Papers

The same can't be said about the related papers of Michael Grinfeld and Pavel Grinfeld, like in *"An Unexpected Paradox in the Kelvin Ponderomotive Force Theory"* [14] where they claim to:

> "*...show that the ubiquitous formula for ponderomotive forces due to a distribution of a polarized substance implies a non-vanishing self-force. This constitutes a striking paradox since this prediction is in startling contrast with observed phenomena.*"
>
> "*...There are a few fascinating exceptions for which F does vanish, including spherically symmetric dipole distributions and constant distributions in elliptical domains.* "

Being mathematicians, apparently they didn't understand that the Kelvin forces don't have to be "*vanishing self-forces".* In fact according to Newton's 3rd law, in electrostatics the volume integral of Kelvin polarization force density in a volume surrounded by a closed conductor surface containing internal charges and an inhomogeneous E-field must not vanish in general. It may vanish only in some specific cases, when all the other electric force types vanish as well. The sum of all different types of electric forces within such volume supposed to be zero (according to the classical EM theory), which includes the electrostatic pressure on the internal boundary surfaces. This error was nicely pointed out by Mr. Cazamias in his response paper of "*A Note on Grinfelds' "Kelvin's Paradox"*" [15].

We highly appreciate any attempt of finding a convincing valid solution to the presented contradictions that are rooted in physical reality, and in which the forces are real physical forces, acting at accurately specified points in space. Just more of the mathematically reverse engineered theories and formulas from axiomatically accepted conservation laws, like the already existing Maxwell stress tensor, and the Korteweg-Helmholtz equation won't resolve the problem of the EM theory's inconsistency. Failing to perform a decent background search of prior art in the field of one's research subject, and/or referring to the already published (most probably also found) sources of ideas and discoveries is not the sign of greatness or originality.

7 APPENDIX B: Construction of the Torsion Pendulum

The construction of a custom built torsion pendulum used in this project is described here. It has got high sensitivity, in the range of 10^{-4} N, and it is able to conduct the HV from the PSU to the thrusters mounted at the beam's moving end with minimum mechanical resistance, while preventing electrical discharges.

DISCLAIMER: The following descriptions are given for information purposes only, and the author does not encourage anyone to replicate this device. For your own safety please don't attempt to replicate and/or use this device unless you are qualified to work with high voltage. An electric shock of sufficient amperage can be lethal. The author cannot be held responsible, and does not assume liability for any damages that could occur to you or your equipment while following the procedures presented in this document. By using the provided information, you accept all responsibility for your actions. I give no warranty on the correctness and usability of the information presented here. Please note however, that these procedures have worked in our case without any damages or problems.

7.1 Measuring the Parameters of Torsion Wire

The torsion pendulum used for the measurement of a torque or force is basically a hanging wire, with a fixed upper end. The measured torque applied to its bottom end twists the wire over a certain angle. If the deformation is less than the elastic limit of the wire, then this angle will be directly proportional to the torque, and the wire's bottom end will rotate back to its original position when the torque is removed (elastic deformation). By measuring the angle of rotation (torsion) we can calculate the measured torque. The correlation between the applied torque M and the angle of rotation φ is $M = D\varphi$. The coefficient D depends on the material, diameter, and length of the wire, and it can be measured directly, or calculated with the formula (G – shearing modulus of the wire's material; r – wire's radius; l – wire length):

$$D = \frac{\pi G r^4}{2l} \tag{24}$$

For these measurements a copper wire of 0.85 mm diameter with enamel insulation was used. The very thin enamel insulation has negligibly small influence on the torsion properties of the wire. Knowing the shearing modulus of copper that is $G = 4.61 \cdot 10^{10}\ N/m^2$ and the length of a sample wire $l = 1.047\ m$ we can calculate the coefficient $D = 2.256 \cdot 10^{-3}\ Nm$.

In order to guarantee the accuracy and reliability of the torque measurement, this theoretical value was confirmed experimentally. For this purpose an acrylic disc of known inertial moment was attached to the bottom of the torsion pendulum wire. The upper end of the wire was embedded into a holder acrylic block that

could be fixed to the ceiling with a screw. The insulation was removed from the end of the wire to establish good electrical contact with the bolt and the GND wire from the PSU for later use. After measuring the natural frequency of the pendulum's oscillation one can calculate the coefficients D and G.

Figure 12: The upper end of the torsion pendulum wire embedded into a holder acrylic block using a bolt & nut (the nut at the top is melted into the plastic and not visible).

Figure 13: The acrylic disc fixed to the bottom end of the torsion pendulum wire and hanged from the ceiling.

Both ends of the wire are bent at 90° (and lead through holes intersecting at 90°) when fixed into the plastic objects with screws to prevent sliding (and dead angle) at very small torsion angles. After fixing the torsion pendulum to the ceiling and straightening the wire, the disc is twisted for about 45° around the wire's axis in horizontal plane, and left to freely oscillate (twist about the vertical axis).

In a 30 second interval 62 to 63 oscillations were counted, which gives a period of T=0.476 to 0.484 second. Since the acrylic flywheel disc assembly is not made of homogeneous material, but it has an extended plastic axis with a screw in its middle, the inertial moments of these components were calculated separately with the following formulas, and added together. Inertial moment of a homogeneous disc or cylinder with radius r and mass m is:

$$J = \frac{mr^2}{2}$$

The inertial moment of a ring or tube with inner and outer radius r_1 and r_2 is:

$$J = \frac{m\left(r_1^2 + r_2^2\right)}{2}$$

The diameter of the disc was 69.5 mm, its thickness was 4.9 mm and the (previously measured) density of the acrylic material was $\rho = 1180\, kg/m^3$. The calculated inertial moment is $J = 1.323 \cdot 10^{-5}\, kgm^2$. Knowing the inertial moment of the disc J and the period of the oscillation T we can verify the validity of the above calculated coefficients D and G using the formulas:

$$T = 2\pi\sqrt{\frac{J}{D}}; \qquad D = J\left(\frac{2\pi}{T}\right)^2$$

Taking the shortest period of T=0.476 s from the measurement we get $D = 2.305 \cdot 10^{-3}\, Nm$, and for the longer period of T=0.484 s we get $D = 2.230 \cdot 10^{-3}\, Nm$, thus the theoretically calculated value of $D = 2.256 \cdot 10^{-3}\, Nm$ is between these two extremes and represents a correct value. This confirms that the shearing modulus of copper is really $G = 4.61 \cdot 10^{10}\, N/m2$, and the formula (24) gives correct results.

7.2 Construction of the Beam and Stabilizer

Knowing the torsional properties of wire, the construction of the thrust measuring instrument could be started. The disc was removed, and the wire was shortened so that after mounting it into a acrylic beam its freely twistable length should be exactly 1 m. The acrylic beam is part of the torsion pendulum that converts a unidirectional force into a torque, which can be measured with the torsion pendulum. The weight of the thruster is balanced with a counter weight on the other side of the beam. If two identical thrusters are used at both ends of the beam, then naturally there is no need for balance weights. The beam is made from a 5 mm thick, 20 mm wide, and 70 cm long acrylic strip.

Figure 14: The acrylic beam with the stabilizer shaft attached to the torsion pendulum wire.

A hole was drilled into the upper center of the beam for the bolt & nut, and another 1 mm thick vertical hole was drilled into the upper edge, so that it merged into the bolt-hole at 90°. The insulation was removed from the end of the wire to ensure good electrical contact with the bolt. The bottom end of the wire was led through this thin tightly fitting hole, and bent at 90° through the bolt-hole in a previously prepared channel

(to leave space for the bolt). The end of the wire was bent into a hook shape and fixed to the beam firmly by the bolt-washer-nut.

Another hole was drilled into the bottom center of the beam, and an M3 thread was drilled into it. A 7 *cm* long stainless steel shaft with M3 thread on both ends was driven into the hole. This shaft acts as a stabilizer when its bottom end is kept in a loosely fitting brass tube 'bearing', and it will also conduct the high voltage from the stator brass tube to the rotatable beam & thrusters.

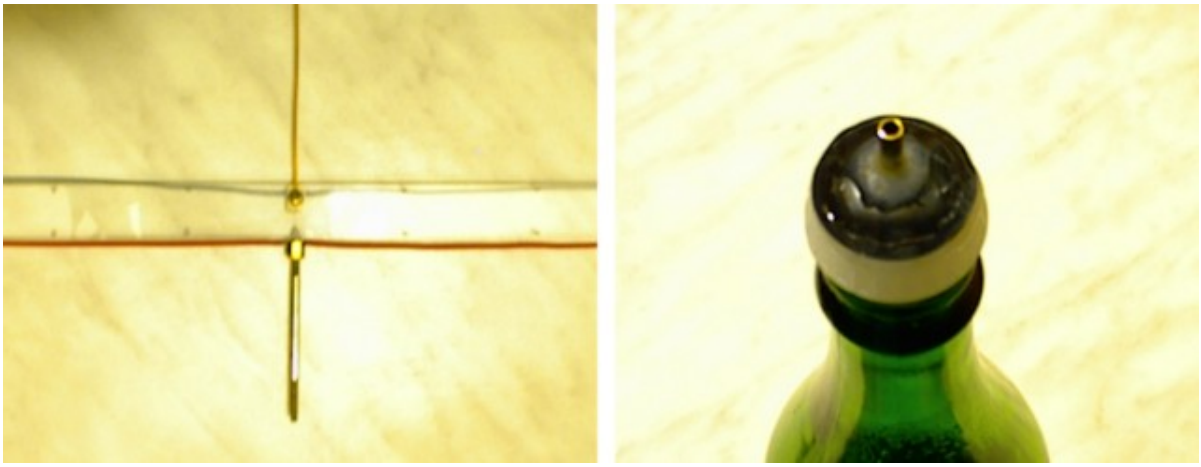

Figure 15: The ground- and HV wires mounted on the beam (left), and the HV contact 'bearing' (right).

The ground terminal of the PSU is attached to the top end of the torsion wire at the ceiling. The horizontal gray wire is electrically connected to the bolt-nut and thus to the GND potential through the torsion wire. The red wire is electrically connected to the stabilizer shaft. About 1-2 *mm* long part of the shaft will hang down into the brass pipe that is glued into a hole on the plastic stopper of a champagne bottle with epoxy glue. The HV cable of the PSU will be connected to this brass pipe and the high voltage is transferred with minimal mechanical resistance. This stabilizer is necessary not only to establish electrical contact, but also to prevent the swinging of the beam. It allows only rotation around the vertical axis and makes the reading of the deflection-angle possible by ensuring that the end of the beam describes a circle around a fixed center.

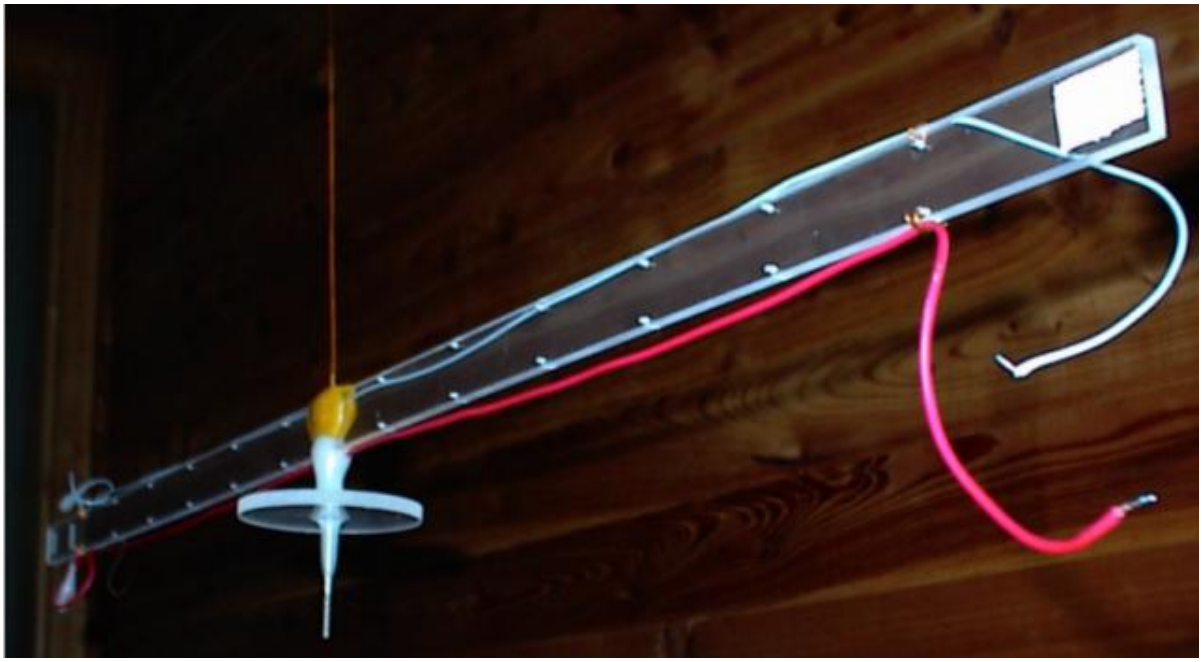

Figure 16: The torsion pendulum with the beam ready for measurements.

Small holes of about 1 *mm* diameter are drilled into the beam near the upper and lower edges at about 5 *cm* spacing to facilitate the fixing the GND and HV wires to the edges, keeping sufficient distance between them

to avoid electrical breakdown of the insulation. In practice it proved to be sufficient if this is done only at the farthest holes using short pieces of the 0.85 *mm* thick enamel insulated copper wire. However, the empty holes are still useful and necessary to serve as points for hanging balance weights. In these experiments only single thrusters were measured, and no HV supply was needed at the other end of the beam, therefore the ends of the wires at the inactive side were insulated with thick paraffin globules to prevent unnecessary current leakage and sparking. This can be done by repeatedly dipping the wire's end into liquid paraffin wax or bee's wax for a very short time, then taking it out and letting it solidify. The thrusters were mostly attached to the end of the beam using strong double-sided adhesive tapes.

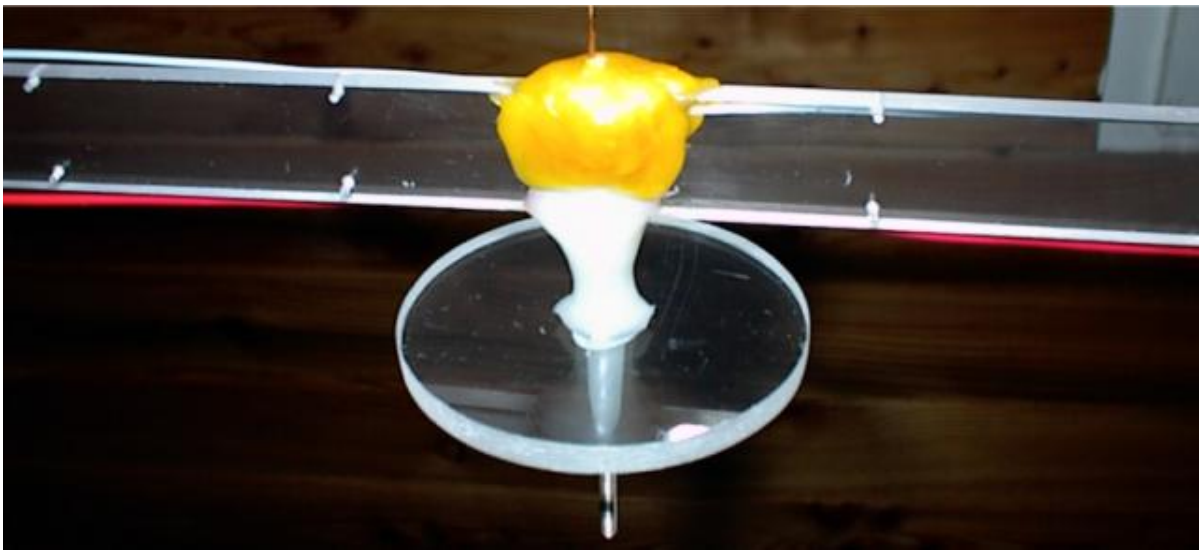

Figure 17: The HV insulation to prevent sparking between the HV shaft and the GND wire.

An acrylic disc of 65 *mm* diameter (can be slightly smaller or greater) was glued onto the shaft to prevent sparking between the GND and HV input terminals. The main upper part of the shaft was coated with thick epoxy glue, but that alone without the disc would not prevent discharges at high voltages. One of the reasons for this is that the small air bubbles that could not be eliminated from the epoxy glue would cause the breakdown of the insulation after a while. The other reason is that the surface resistance and breakdown strength of the epoxy surface is much lower than the bulk values, and sparks were jumping mostly along the surface of the insulation and not along the longer path through the air.

The bolt & nut holding the torsion wire was insulated with bee's wax, because this can be easily removed with a knife if the torsion wire needs to be changed for increased sensitivity. This was done using a 100 *W* soldering gun with a clean copper wire tip. The bee's wax has similarly excellent insulating and breakdown properties as the paraffin wax, but it shrinks less when cooling, it is more elastic, and sticks much better to the surface of other materials than the paraffin. The problem with paraffin is that it shrinks so much during the cooling process that its surface of adhesion to other objects is damaged, and thin discharge paths will appear on the boundary surface between the two materials. This problem is eliminated using bee's wax instead of paraffin.

7.3 The Complete Measurement Setup

The torsion pendulum is prepared for measurement in the following way. The thruster is attached to the active end of the beam. In the example demonstrated on the following picture the thruster is hanged up in line with its center of gravity with the help of an adhesive tape, through a fitting 'window' that was cut into the middle of the tape. At the same time big steel washers (or similar weights) are hanged to the other side of the beam to balance the weight of the thruster. This can be done either by using wire hooks, or long thin bolts driven into the side of the beam. If the thruster's center of gravity is not under the edge of the beam but off on one side, then the counter weights should be hanged to the opposite side of the beam on the passive end to achieve balance not only between the two ends but also between the two sides of the beam. If this would not be done, then the stabilizer shaft would not stand vertically and the mechanical friction in the bearing would be unfavorably increased. A long plastic straw is attached to the active end of the beam with double-sided adhesive tape, to indicate the angle of deflection on a scale placed under its bottom end. More accurate deflection angle measurement is possible using a small mirror attached to the beam center (or shaft) and a laser.

When the beam is balanced, the HV and GND wires on the beam are attached to the electrodes of the thruster and insulated if necessary. The next step is to arrange a table or some kind of stand that would hold the bottle with the brass bearing-tube at appropriate height, and also give place for the scale placed under the indicator straw. The height of the bottle should be adjusted so that the shaft penetrates about 1-2 mm into the bearing tube. The shaft should not hang deeper into the bearing, because that would unnecessarily increase the friction resistance. In order to minimize friction, the bearing should be exactly under the natural rest position of the shaft. If the torsion pendulum is meant to be used as a permanent instrument for multiple use, then it should be installed on a solid and rigid frame instead of the ceiling. In that case the frame can hold the bearing and scale as well.

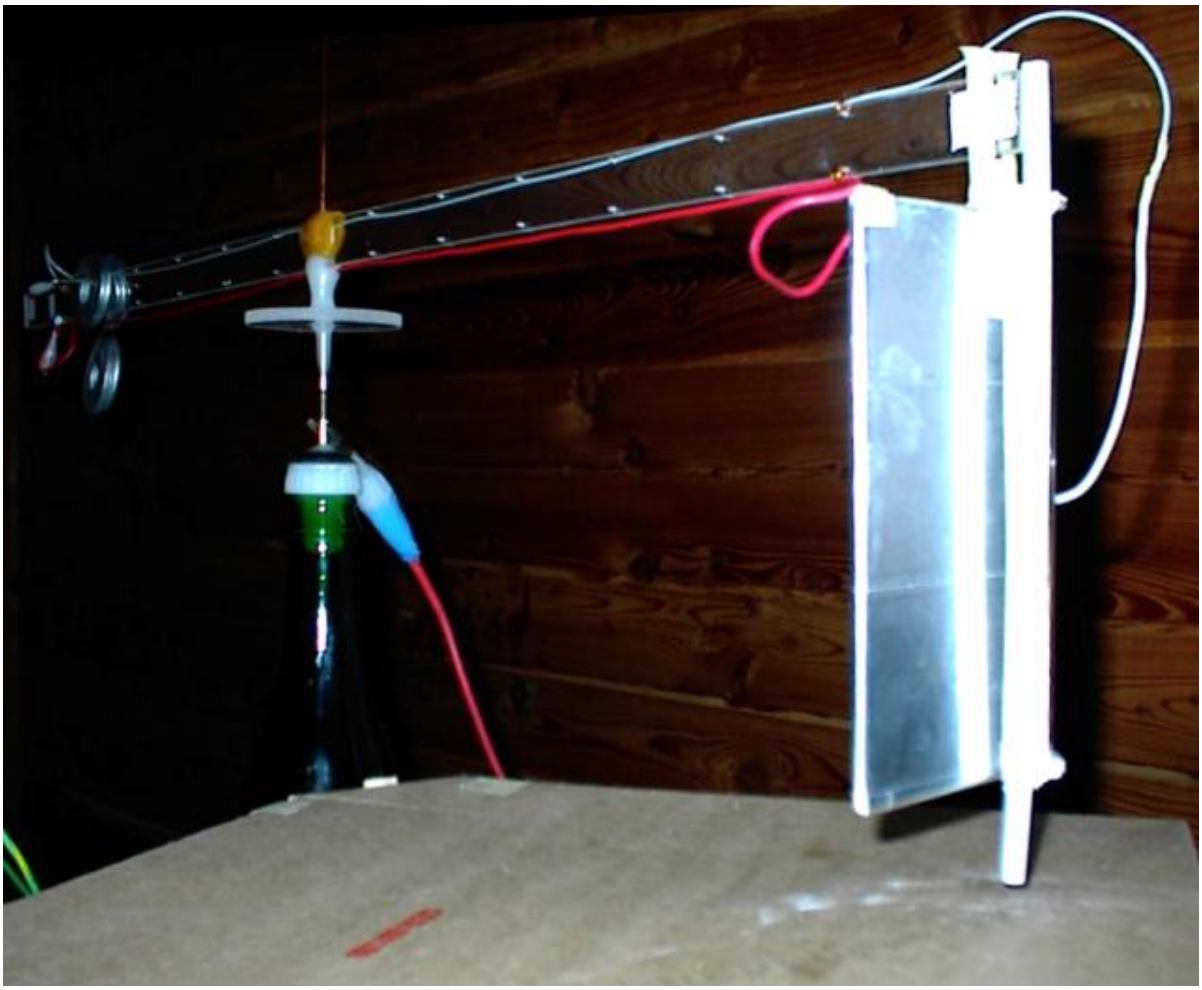

Figure 18: An example of a functional measuring setup (with a different, open thruster).

It is advisable to solder one end of a 5-10 $M\Omega$, 5-10 W resistor in series with the HV cable of the PSU, and a crocodile clip to the resistor's other leg. The junctions and the resistor is coated with a thick layer of silicon rubber glue to provide protective insulation to the resistor, and to give some mechanical rigidity to the junction. This HV terminal is then clipped to the brass pipe. Another insulated wire is electrically connected to the bolt that holds the upper end of the torsion wire at the ceiling, with its other end connected to the ground terminal of the HV PSU.

The scale can be drawn on a cardboard or other insulating sheet of sufficient rigidity. A circular segment is drawn with a radius that is half of the beam's length. Then the arc can be divided into appropriate units (in this case 5 mm divisions) and placed under the straw so that the bottom end of the straw should move above the arc when the beam is rotated. The scale should be insulated from the table with some good thick plastic insulator like a styrofoam sheet. The bottom end of the straw should be about 1-10 mm above the scale, the closer the better, to facilitate accurate reading. When reading the angle of deflection one should keep in mind that the relative position of his eyes to the straw and the scale can have great influence on the accuracy of the reading due to optical reasons. At the same time one should not keep his head too close to the thruster to avoid sparks jumping to his face, and also in order to avoid influencing the measurement results by parasitic electrostatic

attraction between his body and the thruster (if it is open). In case of a completely closed cylindrical thruster, like the one described in this document this is less of an issue.

7.4 Sensitivity of the Pendulum

The sensitivity of the torsion pendulum and the measured forces can be calculated in the following way. We have seen that the torque $M = D\varphi$ and the coefficient D for the copper wire of 0.85 mm diameter and 1 m length can be calculated with the formula (24) to be $D = 2.36 \cdot 10^{-3}\, Nm$.

When observing the deflection, we read an arc length s in millimeters and not the angle of deflection φ. The correlation between the observed arc length of deflection and the active force on the pendulum is:

$$\varphi = \frac{s}{r_i}; \qquad M = Fr_t = D\varphi; \qquad F = \frac{D\varphi}{r_t}$$

$$\boxed{F = \frac{Ds}{r_i r_t}} \tag{25}$$

(where: r_i – radius of the arc movement of the indicator; r_t – distance of the thruster's effective force center from the shaft; F – the measured force).

When $r_i \approx r_t$, the sensitivity of the instrument is about $1.93 \cdot 10^{-4}\, N/cm$ that is more than sufficient to detect the expected thrust predicted by the previous calculations. For a more accurate value of sensitivity, the exact radiuses should be used in the formula (25).

If the thrust causes significant deflection then the voltage should be slowly increased from zero to the desired value to minimize the oscillation of the pendulum, and obtain a stable angle of deflection as fast as possible. If the thrust is too small to cause a well discernible deflection, but we want to be sure whether it really exists or not, then the voltage can be periodically switched on and off synchronously with the natural frequency of the pendulum's oscillation. If the timing is correct and the thrust exists, then the amplitude of the oscillation will increase, confirming the existence of the force. Such small forces can be measured with satisfactory accuracy if the torsion wire is changed to a wire of smaller diameter that will have higher sensitivity.

8 APPENDIX C: Construction of a High Voltage Probe With SMD Resistors

The construction of a custom built HV probe used in this project is described in this section. It was needed for the accurate measurement of primarily DC high voltages using a digital multimeter (DMM) or oscilloscope. Since the commercially available HV probes are fairly expensive and rare to find, it was feasible to build one.

DISCLAIMER: The following descriptions are given for information purposes only, and the author does not encourage anyone to replicate this device. For your own safety please don't attempt to replicate and/or use this device unless you are qualified to work with high voltage. An electric shock of sufficient amperage can be lethal. The author cannot be held responsible, and does not assume liability for any damages that could occur to you or your equipment while following the procedures presented in this document. By using the provided information, you accept all responsibility for your actions. I give no warranty on the correctness and usability of the information presented here. Please note however, that these procedures have worked in our case without any damages or problems.

8.1 The Desired Characteristics for the Design and the Circuit Description

The HV probe had to meet two main requirements, first it had to be fairly accurate (within 5%), and as second it should not demand expensive and hard to find special HV resistors. The primary aim was to make it work reliably at least up to 100 kV but if possible even higher. It should have about $5 G\Omega$ input resistance to minimize the required current, because the voltage of some HV sources drop rapidly with increasing load current. The preferable transfer ratio is 1000:1. In most cases the measured voltage will be less than 30 kV, therefore it is also desirable that it should be as compact as possible to facilitate easy and quick measurements, that would be difficult using big bulky HV probes. It should be well insulated to minimize leakage current through corona discharge. The output connectors should facilitate easy and reliable connections with the standard probes of the DMM and also with the probes of an oscilloscope. The HV probe tip should be changeable and flexible to ensure good contact even when the probe is not held by hand, but placed on a support (unwanted small

vibrations should not brake the contact). The electric circuit diagram of the probe shown on Figure 19 is fairly simple.

Most DMMs and oscilloscopes have an input resistance of 10 $M\Omega$, thus the probe was designed for this load resistance. The 10 $M\Omega$ inner resistance of the attached instrument in parallel with the last 10 $M\Omega$ resistor in the HV probe represent a 5 $M\Omega$ resistance connected in series with the 5 $G\Omega$ resistor chain (500 times 10 $M\Omega$). The instrument measures the voltage drop on this resultant 5 $M\Omega$ output resistance. Since this 5 $M\Omega$ output resistance R_o is 1000 times smaller than the 5 $G\Omega$ resistor chain R_c, there will be 1000 times smaller voltage drop on R_o than on R_c. The transfer ratio is calculated as:

$$\frac{U_{in}}{U_{out}} = \frac{R_c + R_o}{R_o} \approx \frac{R_c}{R_o}$$

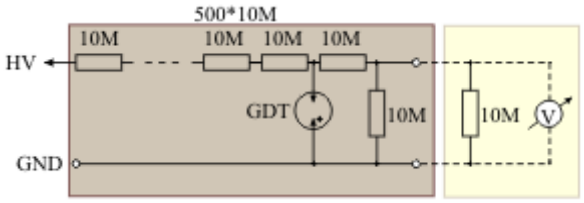

Figure 19: HV probe circuit diagram.

8.2 Choosing the Resistors

In this case the planned transfer ratio is 1001, but in practice we can not obtain exactly 10 $M\Omega$ resistors, because the accuracy of the commercially available resistors is within 20% and 0.1%. Therefore, we can't expect from the initially assembled resistor chain to have a transfer ratio of exactly 1000. The best accuracy can be adjusted empirically after soldering the resistor chain together, and measuring its real resistance. Then according to the measured value, the resistance can be increased or decreased by adding or removing few resistors at the HV end of the chain to obtain the best possible accuracy. Using this approach it is possible to save some money, since we can use the standard 5% tolerance resistors to build a HV probe of the same accuracy that would be possible only using the more expensive 1% (or even more accurate) resistors if we would blindly use the predetermined number (500 pieces) of resistors in the chain.

In order to obtain a compact size, surface mounted (SMD) resistors were chosen. The cheapest SMD resistors fit for the purpose and available in the local electronic-parts shop (in 2003) was the resistor series RC 1206 chip resistor manufactured by YAGEO (www.yageo.com). According to the specification its dimensions are $3.1 \times 1.6 \times 0.55$ mm, and it has a maximum dielectric withstanding voltage of 500 V. Its power rating is 0.25 W, thus the maximal continuous working voltage corresponding to the rated power is $U = \sqrt{P \cdot R} = 1581$ V. Since the electric breakdown voltage of 500 V is the determining limiting factor in this case, we will limit the maximum working voltage to 400 V. This voltage would dissipate 0.016 W that is much less than the allowed max. 0.25 W, and it will allow us to embed the resistor chain into potting resin, which will diminish the heat conduction. At the same time the surrounding resin will increase the breakdown voltage that is beneficial in our case. The used potting materials have a dielectric strength between $10 - 20\,MV/m$, that means the planned approximately 1.5 mm distance between the resistor sections should withstand 15-30 kV. The maximum voltage at this distance will be at two adjacent corners where the resistor chain is folded, i.e. $9 \cdot 400$ V=3.6 kV that is well below the allowed value.

There are even smaller SMD resistors from the same manufacturer like the RC 0603 and RC 0805 series, but these have less breakdown voltage and less rated power, thus they are not fit for our purpose. The smaller dimensions in this case represent a further difficulty in assembling the resistor chain and soldering them together, therefore in this case the RC 1206 is the best choice.

Each resistor can have max 400 V on its terminals and we have 500 pieces in the chain, therefore the maximum voltage that may be applied to the HV probe is $U_{max} = 500 \cdot 400\,V = 200\,kV$. This is well above the desired 100 kV and it represents a satisfactory solution. YAGEO manufactured resistors of the same series up to 22 $M\Omega$, that might occur to be a better choice, since we would need only 227 pieces of 22M, instead of 500 pieces of 10M. This would be cheaper, the resistor chain shorter, and it would require less manual work, but it would be usable only up to $U_{max} = 227 \cdot 400\,V \approx 91\,kV$ which is below the desired voltage limit of 100 kV (besides it was not available at the time). Therefore the 10 $M\Omega$ value is a good choice.

8.3 Over Voltage Protection

To protect the connected instruments from damage in case of internal electric breakdown within the resistor chain, the output voltage was limited with a small gas discharge tube GDT to 200 V. The type 2027-60-B (manufactured by BURNS; www.burns.com) having a rated voltage of 600 V was used. The GDT allows the total voltage on the last 10 $M\Omega$ in the chain (400 V) and the 5 $M\Omega$ (200 V) combined output resistances to rise up to $400 + 200 = 600$ V, while practically conducting no current (and not changing the transfer ratio). But in case the front part of the resistor chain would be shorted with an electric breakdown, it would prevent the voltage to rise above this value. In that case it would conduct the current to the ground and the last two 10 $M\Omega$ resistors in the HV probe would never get overloaded. This way the GDT and the last two resistors will protect the attached instrument.

8.4 The Printed Circuit Board

If compact size is not important, then the resistors can be soldered to the copper traces on the PCB. In this project we were striving for compact size, therefore the resistors were soldered directly to each other, and glued to the PCB. A $340 \times 27 \times 1.5$ mm thick glass fiber PCB was used (with a little wider output end). Almost all the copper was etched away form it except for a small area at the HV end for soldering the tip-holder nut, and the connecting paths at the output where the connectors and the GDT is mounted. The resistor chain was divided into segments, having 4 resistors in straight-line segment, and the fifth resistor connecting each of these segments together. The etched PCB with some sample parts is shown on Figure 20.

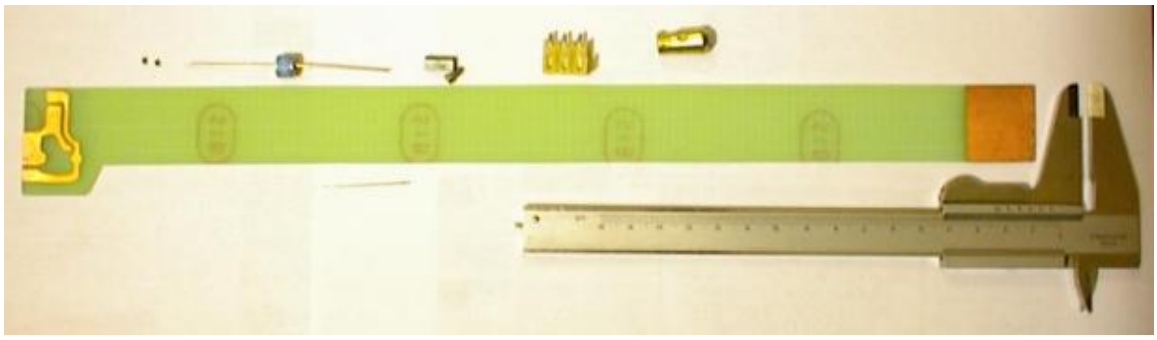

Figure 20: The etched PCP with sample parts.

The copper pattern on the left (output) side should not be copied from the photo, because it was designed to connect the GDT parallel with the output terminals, and not as shown on the above discussed diagram. This does not provide the best protection, and it was made only for test purposes. The best is if one uses the circuit diagram described above, and designs the PCB accordingly.

Two different parallel output connectors were built in. One for the DMM probes that provide a tight fit for simple insertion, and another (made of small brass connectors used in electric installations) specially fit for the hook-type probes of an oscilloscope. Both connector types have 3 poles: one for the signal output, one for the instrument ground, and one for the input ground. The connectors for the scope can also be used for other types of connections since it can receive a 3mm thick wire, which can be fixed in place with bolts if needed. When the fixing bolts are removed, the holes represent ideal contacts for hooking the scope probes into them as shown on Figure 26.

8.5 Mounting the Parts on the PCB Prior to Soldering

After etching the PCB, lines were scratched (drawn) on it with a needle to mark how the resistors should be aligned. Don't use graphite pencil to avoid slightly conductive graphite paths, which could create short circuits at high voltages. Then the area of the resistor chain was coated with a thin layer of two-component epoxy glue. Best is to use a type with long working time of about 2 hours. If the pot life of the glue is shorter, then only a small part of the area should be covered at a time. The resistors are placed on this glue surface along the marked lines touching each other's terminals. After mounting the resistors onto the PCB it should be kept on a dust-free place to cure.

8.6 Soldering

After the glue is cured one can start the soldering. A sharp pointed soldering-iron tip is required for this operation. One should take care that the temperature of the tip is not too high to overheat the tiny resistors. The soldering of one joint should take only few seconds, not to damage the chips.

An alternative solution that would substitute the sensitive soldering is to cover and connect the contacting terminals of the resistors with a tiny dot of some reliable conductive paint. A conductive paint fit for this purpose is for example the one used in car repair workshops to repair the broken heater resistor lines in windshields. It can be found in special paint shops and it is fairly expensive, but since we need very small quantities it can be affordable. The picture of the HV probe panel with mounted and soldered components is shown on Figure 21.

Figure 21: The PCB with mounted parts and soldered resistor-chain.

After soldering, the resistor chain has to be checked whether all the soldered joints conduct properly or there are some poor contacts. This can be done with a DMM switched to high resistance range. Although in this example the highest range of the DMM was $4\,G\Omega$ that would theoretically allow us to measure the resistance of the chain in two parts (ex. $2 \times 2.5\,G\Omega$), in practice the instrument was not sufficiently accurate in this range. The practical solution is to use the $40\,M\Omega$ range, and measure 3 successive resistors in series at a time. This requires about 166 measurements that is fairly time consuming but it gives accurate and reliable results. After adding together the measured partial resistances, we get the total resistance of the chain, which should be about $5\,G\Omega$. If it is higher, then one can remove some resistors from the HV end of the chain; or if it is less, then some more can be added. When adding or replacing only few resistors, it is faster and better to use a universal instant adhesive like Loctite's Super Attack.

8.7 Measuring and Calibrating the Resistor Chain

The final length of the resistor chain is preferably determined by measuring a sufficiently high DC voltage that is reliably and accurately measurable at the output of the HV probe. If there is no fault in the soldering then the tiresome series of measurements described in the previous section can be avoided, because this approach will yield the same result. The above series of measurements is unavoidable only if there are faults in the soldering, and these faulty joints have to be found.

The simplest method of calibration would be to measure the mains AC voltage ($\sim 220 - 230\,V$) through the HV probe and also directly with the DMM, and calculate the transfer ratio by dividing the second value with the first one. Unfortunately this simple approach would yield unreliable results, because the unshielded HV probe acts as an antenna, and a few hundred mV of 50 Hz AC signal will be induced in it (mainly capacitively) by the live electric cables in the house. This induced signal would get superposed over the voltage (of same frequency) that was intended to be measured, and it would falsify the results. We wouldn't know for sure what part of the measured voltage is the induced disturbance signal, and what part is the transferred voltage from the HV tip. For this reason DC voltage is needed for the calibration.

The simplest electric circuit for such a DC measurement setup is shown on Figure 22. The diode with a capacitor represents a simple rectifier circuit. The DC voltage on the HV terminal will be approximately $\sqrt{2}\,U_{eff}$ that is about 311 V when $U_{eff} = 220$ V, and negligibly small current will be drawn from it by the probe. These voltages and the available current intensities are hazardous to life, only qualified people should perform these measurements!

First the neutral contact of the power socket has to be identified. This is done by measuring the AC voltage between the ground contact and the examined socket contact with a DMM. The one that shows about 220 V AC (or 110 V in some countries) is the live contact, and this should never be touched with bare hands because it can kill. The contact that shows nearly 0 V or only few volts relative to the GND is the neutral. It is very important that the neutral should be connected to the bottom of the capacitor and to the GND contact of the HV probe, and not the live contact (phase) of the socket! The live contact should be connected only to the left side of the diode and never touched!

When the rectifier circuit is connected to the mains voltage, the DC voltage on the capacitor is measured directly with the DMM. This supposed to be about 311 V in Europe or 155 V in some other countries. Next,

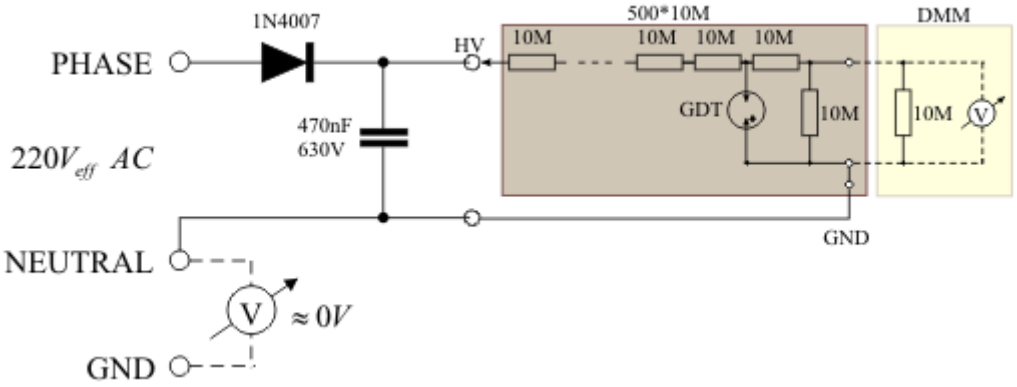

Figure 22: DC Calibration circuit of the HV probe.

the HV probe is connected as shown on Figure 22, and the DMM is connected to its output terminals. If the HV probe works properly then the DMM should indicate 1000 times lover voltage, i.e. about 0.31 V (or 0.15 V) DC. If the accuracy of transfer ratio is unsatisfactory, then one can try to move the HV input connection point up or down on the resistor chain until the desired ratio is obtained. This might require adding some more resistors, but more often to remove few pieces. It is important that after disconnecting the rectifier circuit from the mains voltage, the capacitor should be discharged with a few $k\Omega$ resistor, because it contains significant energy at a dangerous high voltage. Do not touch its terminals!

If multiple stages of Villard (Cocroft-Walton) type voltage multiplier is used instead of the above simple half wave rectifier to obtain higher voltage, it can falsify the measurement results. The reason for this is that the output voltage of this multiplier drops rapidly with the increase of the load current and the number of stages. The real output voltage will be less than the theoretical $U_{out} = 2nU_p$ (where n is the number of stages, and U_p is the peak input voltage) with the voltage drop that is calculated as (I – load current; C – capacitance of the capacitors; f – frequency of the input AC voltage):

$$U_{drop} = \frac{I}{Cf}\left(\frac{2}{3}n^3 + \frac{1}{2}n^2 - \frac{1}{6}n\right)$$

Since the frequency of the mains voltage is very low (about 50-60 Hz), and the practically applicable capacitances for high voltages have also small values, even 2-3 stages of the multiplier can cause a significant voltage drop when directly loaded with the 10 $M\Omega$ internal resistance of the DMM. In this case the DMM does not measure the theoretical U_{out} voltage that supposed to be present when no current is drawn, but a value that is U_{drop} less than that. When the same voltage is measured through the HV probe that has 1000 times greater input resistance (and draws 1000 times less load current I) we will measure a higher value that is closer to the theoretical unloaded voltage. Since the direct measurement with the DMM can not provide an accurate reference voltage to serve as a base of comparison, it is best to use some other type of DC voltage source for the adjustment, which is less sensitive to the load current.

8.8 Connectors and the HV Probe Tip

After finalizing the resistor chain, a brass nut was soldered to the HV end of the PCB that can hold the changeable HV tips, and the excess PCB and copper layer was cut off. The nut is connected to the first resistor with a short wire. The connector for the DMM probe tips was soldered to the PCB, and the other type of brass connector elements were fixed to the PCB with small screws and also soldered (for better electrical contact).

A flexible and elastic HV probe tip was made from the pleated shield of a shielded cable. The sample piece was taken from the shielded cable of an old monitor that connects it to the PC, but other cables may have similarly good shielding. A piece of this cable was cut off, the inner wires were pulled out from the shielding, and the plastic insulation was removed. Then it was cut to the desired length and a short piece of brass bolt with rounded end was pushed into one of its ends, and soldered to the shield. About 2 cm threaded piece of the same bolt was fitted into the other end of the shield and soldered, so that about 1.5 cm of undamaged threaded part of the bolt should be free. This part can be screwed into the nut on the PCB (see the photos). The solderings should be filed to eliminate sharp edges to prevent corona discharge. The advantage of this probe tip is that its elasticity can maintain good contact with the probed surface even in the presence of small vibrations. A rigid probe tip is separated immediately from the contact surface at the slightest movement.

Figure 23: The flexible HV probe tip.

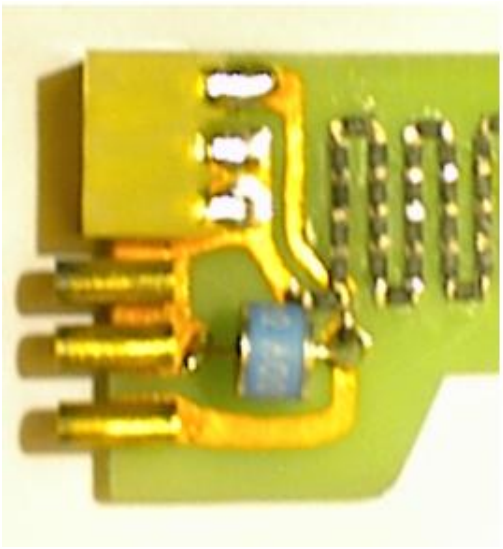

Figure 24: The output connectors and the tip holder brass nut.

8.9 Potting the HV Probe

After finalizing the electronics on the PCB, the whole probe was potted with a potting compound of high resistivity and high dielectric strength. There are several good materials for this purpose but preferably those with low shrinking percentage are the best. In the present example water clear transparent polyester resin was used, because it has low shrinkage, good insulating and breakdown properties, and any bubbles or internal breakdown is visible through the material. The thickness of the insulating layer is about 8-10 mm, that can withstand about 80-200 kV potential difference depending on the type of the potting compound (the thickness of this layer can be increased if necessary).

Before pouring the resin, the openings of the connectors and the nut were sealed with some insulating adhesive tape to stop the leakage of resin, as shown on Figure 25. Then a pot was made from 5 mm thick transparent acrylic sheet, glued together with instant adhesive, which held the resin and gave form to the HV probe. The PCB was placed into the pot, and resin was poured over it. This operation should be done with care to prevent air bubbles from being trapped beneath the PCB or anywhere else in the resin. The air bubbles diminish the dielectric strength of the insulation. The elimination of small bubbles can be accelerated if the brush is removed from an electric toothbrush, and the vibrating end is held against the side of the pot.

When the resin has hardened, the small front and back walls of the mould were removed to free the openings of the nut and connectors, but the rest of the acrylic pot was kept as part of the HV probe. After cleaning some additional epoxy glue was poured over the DMM connector and the GDT to improve mechanical strength and to obtain a little thicker insulation.

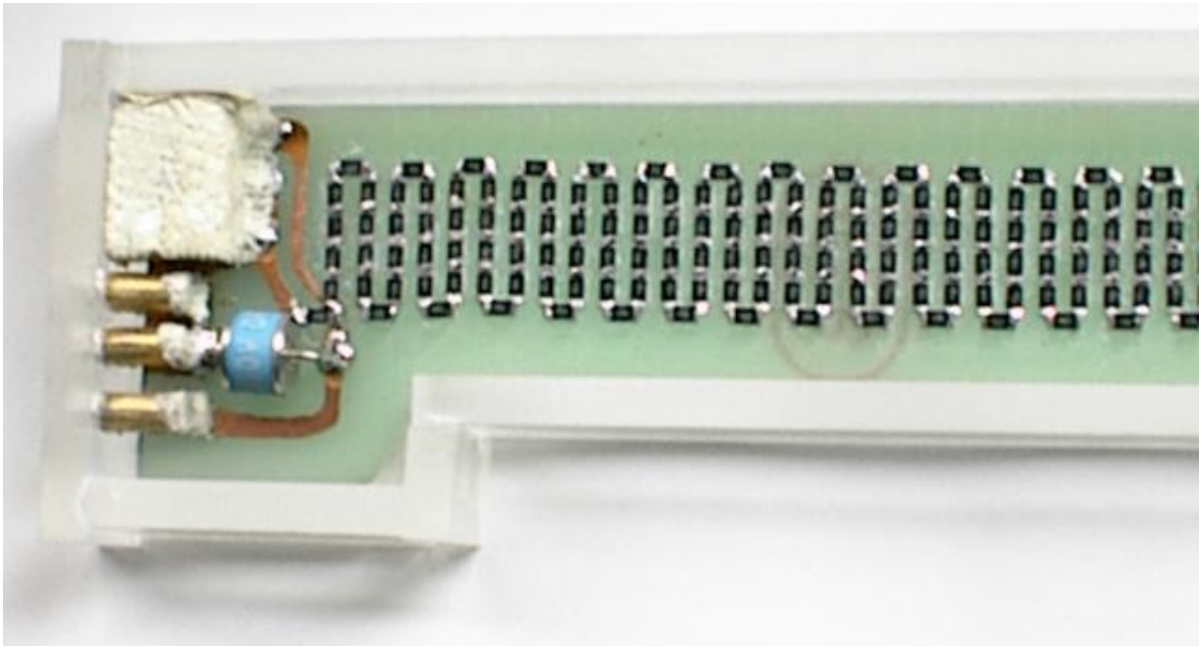

Figure 25: The PCB within the acrylic pot with sealed connector openings.

8.10 Final Testing and Measurements

The HV probe was now ready, and the final testing could be performed. The transfer ratio was measured according to the earlier description, using a half wave rectifier as shown on Figure 22. The directly measured voltage was 320 V DC (the mains voltage was higher than 220 V AC), while the voltage measured through the HV probe was 0.318 V DC. This represents a transfer ratio of 1006:1 which is about 0.6% deviation from the theoretical 1000:1 ratio, and it is satisfactory.

This transfer ratio is valid only for DC or low frequency AC voltages, and it changes with increasing frequency due to parasitic capacitances. Since the attenuation is different for different frequencies, the non-sinusoidal waveforms (especially those with sharp rise and fall edges) are somewhat distorted. For accurate high frequency, high voltage measurements other types of shielded special HV probes should be used (mainly using precise capacitive voltage attenuation). However, if no high precision is required, then with extra shielding added, and frequency characteristic of the HV probe recorded (transfer ratio vs. frequency), it can be used even for the measurement of higher frequency sinusoidal waveforms by using the measured transfer ratio curve (instead of the 1006:1 at DC).

When the HV probe is not connected to the rectifier the induced parasitic 50 Hz AC disturbance signal had an amplitude of about 0.2 V. This value depends on the distance of the probe from live power cords. When a capacitor of 0.04 μF was connected between the output and GND terminal of the probe, this signal decreased to only few mV pulses originating from the voltage multiplier operating near the HV probe tip (but not connected). These waveforms are shown on Figure 27.

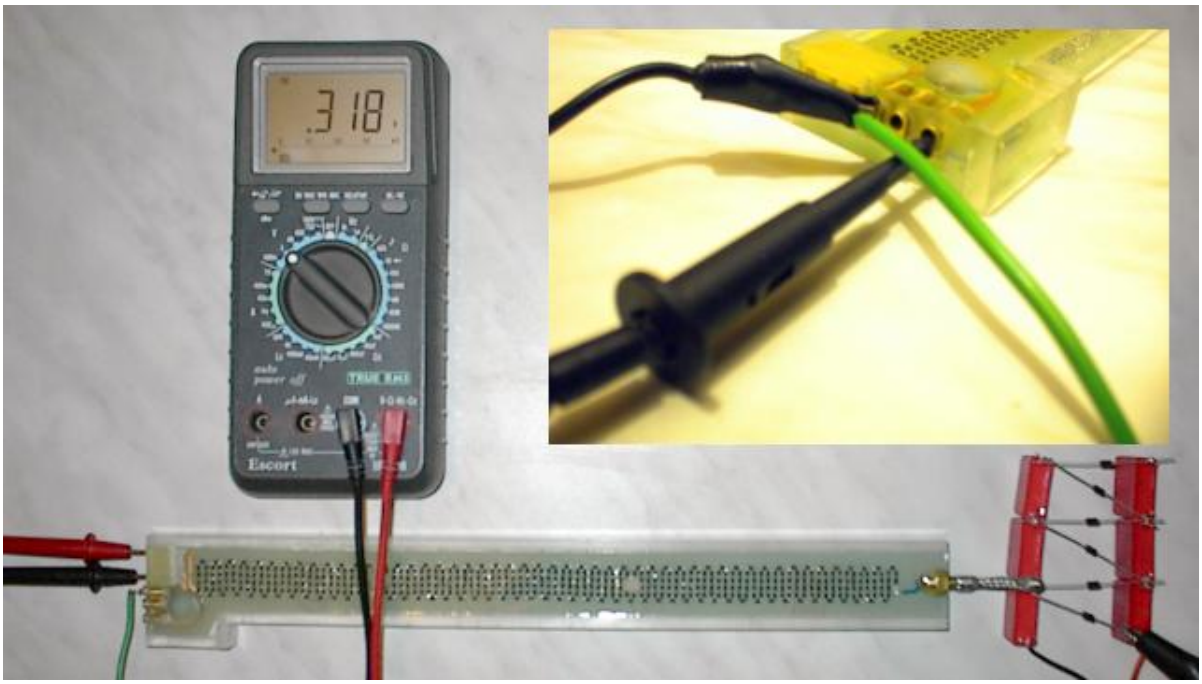

Figure 26: Checking the transfer ratio of the probe (0.318 V is indicated), and an illustration of the oscilloscope's probe being hooked onto the output connector through the screw-holes at the bottom.

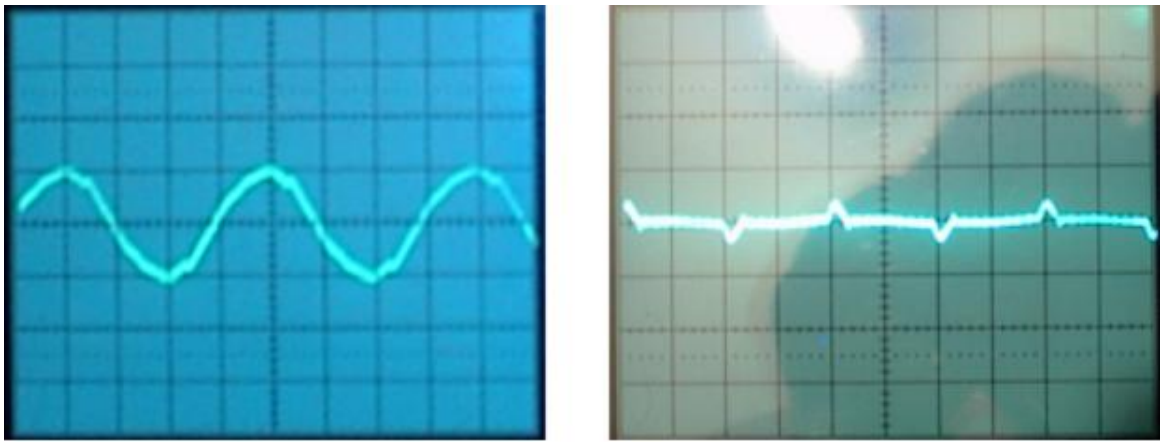

Figure 27: The parasitic 50 Hz signal with disconnected HV probe tip (left); and the same measurement when the output is filtered with a parallel capacitor (right); (0.2 V/div; 5 ms/div).

The output signal of the unshielded and unfiltered HV probe measuring the 320 V DC on the rectifier is shown on the left of Figure 28. The 50 Hz AC parasitic signal is riding on the DC voltage of 0.318 V as measured with DMM. When the filtering capacitor is connected to the output, the shape of the signal significantly smoothed out, and the DC voltage was clearly visible (right).

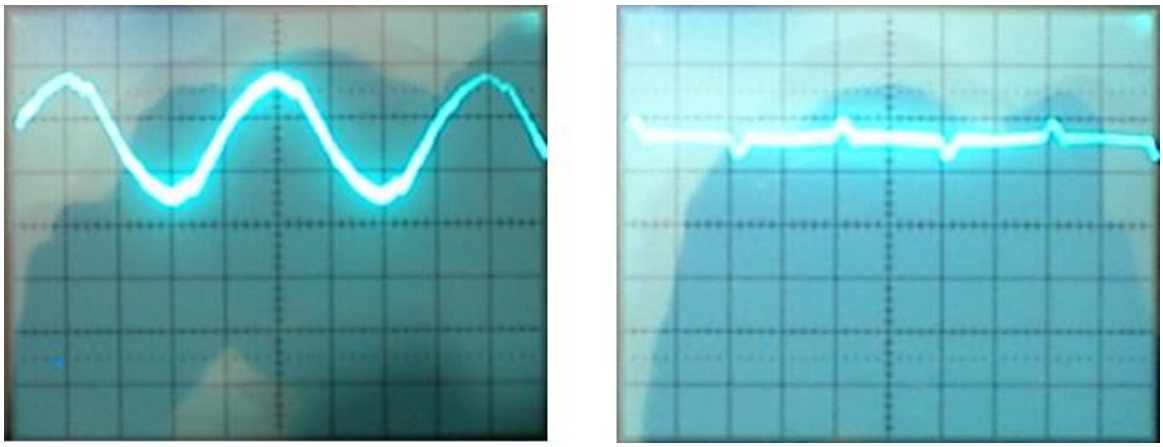

Figure 28: The unfiltered and the filtered output signal shapes of the probe when measuring the 320 V DC on the rectifier (0.2 V/div; 5 ms/div).

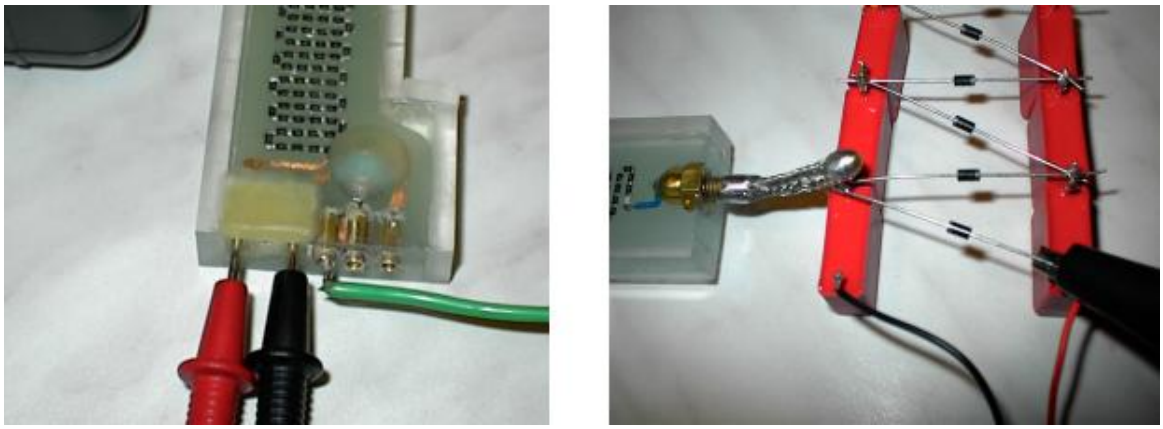

Figure 29: The standard DMM probe tips tightly fit in the connectors, and the elastic HV probe tip touching the test point on the rectifier.

Finally it is important to note that since the resistance of the resistor chain in the HV probe is about 5 $G\Omega$ that is a very big value, it is very sensitive to any contamination or moisture that might come to the surface of the probe. The internal resistance of the resin is much greater than this 5 $G\Omega$ and it will not influence the functioning of the probe. But dust, moisture, or similar contaminations can create a resistive path from the HV tip to the output on the surface of the HV probe, which is in the range of several $G\Omega s$. This would represent an extra, unwanted resistor connected in parallel with the 5 $G\Omega$ resistor chain, and thus falsifying the measurement results. Such unwanted contamination can alter the measurement results even if it is not visible with naked eyes. So the only way to be sure that after a long time period of storage the HV probe did not lose its accuracy is by performing the above test, and cleaning its surface if necessary. The surface contamination is also dangerous at very high voltages, since in most cases the bulk resin will withstand the intense E-field, but surface discharge may occur on its surface, mainly caused by impurities. When such very high voltages are measured, it might be necessary to extend the HV probe with a long insulated adapter-tip (with a sealed fit at the nut), and the whole probe can be mounted into a thicker PVC pipe (which is not touching the HV end of the probe) to minimize the risk of surface conduction and discharge.

It is also important to know that the GDT can protect the attached instruments from over voltage only if the external ground is connected to the HV probe! If this is forgotten, or the connection is accidentally broken while the HV probe tip is connected to high voltage, the same HV potential is transferred to the instrument, and it will "float". This can damage the instrument. The user has to make sure that the HV probe is always firmly connected to a proper external grounding while it is connected to high voltage.

References

[1] Frisch, M. 2005. Inconsistency, Asymmetry, and Non-Locality: A Philosophical Investigation of Classical Electromagnetism. Oxford: Oxford University Press. 8

[2] Belot, Gordon (2006) Is Classical Electrodynamics an Inconsistent Theory? 8

[3] Haus, Hermann A., and James R. Melcher , Electromagnetic Fields and Energy . (Massachusetts Institute of Technology: MIT OpenCourseWare). http://ocw.mit.edu (accessed 11.09.18). License: Creative Commons Attribution - NonC ommercial - Share Alike. Also available from Prentice - Hall: Englewood Cliffs, NJ, 1989. ISBN: 9780132490207. 8

[4] Dr. Branko Popovic, Electromagnetika. Univerzitet u Beogradu. Gradevinska Knjiga, Beograd, 1980, p.102-108.

[5] F. W. Peek, Dielectric Phenomena in High-Voltage Engineering, McGraw-Hill and Co., New York, 1929. 19

[6] Pellat H 1895 Mesure de la force agissant sur les dielectriques liquides non electrises places dans un champ elitrique, C. R. Acad. Sci., Paris 119 691–4

[7] T. B. Jones, M. P. Perry, and J. R. Melcher, Dielectric Siphons, Science 174, 1232 1971.

[8] T. B. Jones, J., Liquid dielectrophoresis on the microscale, Electrost. 51–52, 290 2001

[9] Penfield, P. A., and Haus, H. A., 1967, Electrodynamics of Moving Media, MIT, Cambridge. 15

[10] Stratton, J. A., 1941, Electromagnetic Theory, McGraw-Hill, New York 15

[11] Woodson, H. H., and Melcher, J. R., 1968, Electromechanical Dynamics, Part I: Discrete Systems, Wiley, New York 15

[12] D. Wijesinghe, D. Nawarathna, Design of a Dielectrophoretic Based Micropipette for Gene Expression Applications Using COMSOL 20

[13] B Jones, T & Gram, Roger & Kentch, Kyle & Harding, D.R.. (2009). Capillarity and dielectrophoresis of liquid deuterium. J. Phys. D: Appl. Phys. 42. 225505-9. 10.1088/0022-3727/42/22/225505. 20

[14] Grinfeld, Michael & Grinfeld, Pavel. (2015). An Unexpected Paradox in the Kelvin Ponderomotive Force Theory. Results in Physics. 81. 10.1016/j.rinp.2015.03.004. 22

[15] James Cazamias, A Note on Grinfelds' "Kelvin's Paradox", Weapons and Materials Research Directorate, ARL. 23

[16] K. Simonyi, Villamossagtan, Akademia Kiado, Budapest, 1983 ISBN 963 05 3413 4

[17] K. Simonyi, Elmeleti Villamossagtan, Tankonyvkiado, Budapest, 1981 ISBN 963 17 5272 0

[18] J. D. Jackson, Classical Electrodynamics, 3rd Ed., John Wiley & Sons, Inc. 1999 ISBN 0-471-30932-X

[19] G. A. Korn, T. M. Korn, Matematikai Kezikonyv Muszakiaknak, Muszaki Konyvkiado, Budapest, 1975, ISBN 963 10 0673 5 (Original Title: Mathematical Handbook for Scientists and Engineers, 2nd Ed.)